ENERGY ABSORPTION METHODS FOR FLUID QUANTITY GAUGING IN LOW GRAVITY

by

EDWARD BIJAN BOKHOUR

B.A., Queens College of the City University of New York

(1978)

Submitted in Partial Fulfillment of the Requirements for the Degree of

MASTER OF SCIENCE IN
AERONAUTICS AND ASTRONAUTICS

at the

MASSACHUSETTS INSTITUTE OF TECHNOLOGY
June 1988

Signature of Author _____
Department of Aeronautics and Astronautics
May 6, 1988

Certified By _____
Professor R. John Hansman
Thesis Supervisor, Department of Aeronautics and Astronautics

Accepted By _____
Professor Harold Y. Wachman
Chairman, Department Graduate Committee

ENERGY ABSORPTION METHODS FOR FLUID QUANTITY GAUGING IN LOW GRAVITY

by

EDWARD BIJAN BOKHOUR

Submitted to the Department of Aeronautics and Astronautics on May 6, 1988
in partial fulfillment of the requirements for the
Degree of Master of Science in Aeronautics and Astronautics

ABSTRACT

Two electromagnetic energy absorption approaches to gauging fluid volume in low gravity were presented and experimentally tested. Both approaches infer fluid volume from losses in the fluid determined from measurements of the quality factor of the tank-fluid system. Quality factor was related to fluid volume, dielectric constant, and loss tangent.

In the first method, loss is determined at resonance in a coaxial right circular cylindrical tank at a number of resonant frequencies in the microwave region. The results of these measurements were averaged to reduce fluid orientation dependance due to resonant electric field structure within the test tank. Test fluids were kerosene and ethyl alcohol, chosen to simulate the electromagnetic behavior of liquid oxygen and liquid hydrogen. In the second method, loss was determined below any electromagnetic resonance in a parallel plate capacitor. Electric field inside the tank was quasi-static, and nearly uniform. Foam was used to simulate liquid oxygen and liquid hydrogen in a variety of configurations within the tank.

The results for the first method showed that averaging reduces fluid orientation dependance due to resonant field non-uniformities. The results for the second method showed substantial orientation independance for many foam configurations.

Thesis Supervisor: Dr. R. John Hansman
Title: Professor of Aeronautics and Astronautics

Acknowledgements

The author wishes to gratefully acknowledge the guidance of Professor R. John Hansman in the preparation of this thesis. Extra special thanks are given to Barbara Goldberger, for the years of patience and understanding.

Thanks are also due to the brave men and women of the Aerodrome at 37-442. The legacy lives, and the motto stands: "Non injuriat est, sportatus continuum".

This thesis is lovingly dedicated to Ehsan Bokhour and the Bokhour family, without whose understanding and support this rather remarkable chapter of my life would not have been possible.

Table of Contents

Chapter 1

Introduction

1.1 Overview

Increased accuracy in the determination of fluid quantity in low gravity will be required for many future space missions. Proposed vehicles such as the Orbital Transfer Vehicle (OTV) will demand accurate propellant gauging for efficient refueling from orbitting platforms. Orbital maneuvering vehicles will also require resupply of fuel. In addition, geosynchronous satellites now demand precise knowledge of propellant quantity in order to extend operational life, due to orbit clearing requirements.

In general, present technology will not reach the 1-3% target accuracy generally thought necessary for fluid quantity gauging. The cost of this inaccuracy can be substantial. For example, gauging inaccuracies during refueling by the OTV would require carrying extra fuel to geosychronous orbit, thus reducing payload. For satellites, enough fuel must be retained at the end of operational life to perform the de-orbit maneuvers. Propellant volume uncertainty thus means ending operational life earlier than if precise gauging were possible.

There are many potential techniques for determining fluid quantity aboard spacecraft. As an example, the Space Shuttle Orbiter uses several measurement methods. The Orbital Maneuvering System (OMS) uses capacitive gauging during thrust phases. The two storable propellants, monomethyl hydrazine and nitrogen tetroxide, are measured with accuracy on the order of $\pm$ 5%. The Reaction Control System (RCS) is also a bipropellant system. Gauging is accomplished using a combination of Pressure-Volume-Temperature (PVT) and analytical burn time integration techniques which together achieve accuracy as low as 3% for short duration missions. The electrical system uses liquid oxygen and hydrogen stored in the supercritical (high pressure, single phase) state, which allows capacitive gauging to be used, and achieves accuracy on the order of 5%.

Proposed spacecraft designs call for increased reliance on cryogenic propellants. Improved accuracy in the gauging of these fluids will be difficult using presently available technology. For example, vehicles such as the OTV will require the use of high specific impulse fuel, such as the liquid oxygen-liquid hydrogen combination. Although capacitive gauging can be used if these fluids are stored in a single phase (i.e. uniform density), the high pressures required impose a severe weight penalty when considered for larger tanks. Sub-critical storage eases these restrictions, but requires gauging of the fluid in two phases. In low gravity, capillary forces will dominate fluid behavior and cause difficulties for conventional capacitive gauges.

In general, uncertainty in fluid orientation, the use of cryogenics, and the need to increase gauging accuracy without extensive hardware or ground support make currently available methods of fluid quantity measurement inadequate. Thus, a new technique is needed which addresses the requirements of the next generation of space vehicles.

This thesis proposes two approaches which both use electromagnetic energy absorption in the tank as an indication of fluid volume. These have the potential to be insensitive to fluid orientation, and can be applied to two phase liquid oxygen and liquid hydrogen measurement.

The primary problem faced in low gravity fluid gauging results from the behavior of fluids in low gravity. This behavior is discussed in Appendix B. Ambiguities in fluid orientation, density and phase make reliable determination of the physical state of the fluid difficult. Cryogenic temperatures present additional sensor technology challenges.

Potential gauging systems can devided into three general types: point, line, and volume. Point type systems determine quantity at each of a number of points distributed throughout the tank. An example is a capacitance grid, made up of wires strung across the tank at regular intervals. These quickly become heavy and complex with large tanks, and suffer from fluid adhesion to the sensors due to capillary forces in the fluid at low gravity.

Line type systems have fewer components, and function by determining fluid quantity along a particular line through the tank. Methods involving nuclear sources are generally of this type. The density of fluid along a line-of-sight is determined by radiation attenuation. Accurate gauging usually requires a number of sensors, and volume is inferred from the combined attenuation measurements. The large number of sensors required and the potential radiation hazards prevent this type of system from being commonly used.

Pressure-Volume-Temperature (PVT), Radio Frequency (RF), and infrasonic gauges are examples of volume type gauging systems. These systems generally have a single sensor which communicates with the entire tank volume, either by mechanical or electromagnetic means. The single sensor makes these gauges simpler, and they are therefore preferred over point and line type systems.

Numerous techniques for determining fluid volume in low gravity have been studied. However, many of these studies were devoted to specific spacecraft or systems, and cannot be used for missions involving cryogenic propellants. The methods presently considered viable for these applications are Radio-Frequency, PVT, and ultrasonic gauging.

PVT methods use the ideal gas law to relate known tank volume changes to measured pressure changes. These are generally position independant, provided the fluid is isolated from the sensing instrument in the tank. However, when a step volume change is applied, pressure measurements cannot be simply related to fluid volume until there is a uniform temperature distribution in the tank. This requires long stabilization times. New approaches are presently under investigation which address this difficulty by applying an oscillatory volume change.

Ultrasonic ranging techniques use sensors located on the tank walls which determine the distance, in a particular direction, from the detector to the nearest fluid-vapor boundary. If the detector is submerged, the distance to the nearest vapor bubble will be measured. Use of a number of sensors allows estimation of the ullage bubble size, from which fluid volume can be determined. This method works well if the ullage is restricted to a simple configuration, such as during thrust or for large tanks when accelerational forces dominate fluid behavior.

Radio frequency methods of determining fluid quantity in low gravity have been under investigation since about 1962. The majority of this work has been done by Bendix Corp. Instruments and Life Support Division [1, 2]. Other work in this field has also been done by the National Bureau of Standards [3]. The work at Bendix has recently been extended by Ball Aerospace [4].

In general, there have been three approaches to this problem, each involving measurement of the response of the fluid-tank combination to illumination of the contents with electromagnetic energy. These approaches relate impedance, resonant frequency, and energy absorption to fluid volume.

The first method, studied by Bendix, input RF energy to the tank via a small antenna [5, 6, 7]. The report claims uniform illumination of a cigar shaped tank with this antenna. This was accomplished by driving the antenna at frequencies well above

the fundamental resonance frequency of the tank. The electrical loading (i.e. impedance) of the antenna was related to the fill level. Although three methods were tested (the difference being essentially signal processing changes), the method with the best results predicted ± 0.5% accuracy with the fluids N_2O_4, Aerozine, and monomethyl hydrazine. The system was intended for use in the Apollo fuel tanks. Extension of the concept to larger tanks and cryogenic systems was not done, although substantial position independance was claimed.

The second method, investigated by the NBS, uses the principle that the resonant frequency of the tank will change in proportion to the fluid mass in the tank. Tests were performed on supercritical liquid hydrogen and nitrogen in normal gravity. While the concept was demonstrated feasible in 1-G, the distortion of mode shapes and the resulting resonant frequency shifts caused by fluid slosh and interface configurations in subcritical (two phase) fluids would prevent this method from being used in low-g. In general, since resonant frequency depends on tank geometry and fluid location in addition to fluid mass, any gauging method which depends on frequency measurement will be sensitive to fluid orientation.

Bendix approached the resonant frequency versus mass problem by counting the number of resonance modes in a prescribed frequency region [8, 9]. As the tank is filled, all the resonances shift down in frequency. Since higher order modes are spaced more closely together, the total mode count rises with fill level.

A breadboard system using this method was assembled and tested at zero-g aboard the KC-135 aircraft, using Benzine as a test fluid. LO_2 and LH_2 were tested on the ground in various tank orientations. The results were a mean error in LH_2 measurements of 2.18% with 75% of the data having <3% error, and a mean error in LO_2 measurements of 0.898% with 90% of the data having <2% error. On the basis of both the zero-g and ground tests, the report concluded that the method was insensitive to fluid motion within the stated errors. However, complexity in the analysis and the uncertainty in mode count caused by noise and 'mode degeneracy' (overlapping and non-linear shifting) probably prevented this method from being fully developed.

One improvement to the frequency shift method presently under investigation involves averaging of resonant frequency shifts for the first few resonance modes. This approach acknowledges that the electric field structure is not uniform throughout the tank at any one of these frequencies, but strives to average the results from a number of modes to compensate for the inherent position dependance. Preliminary testing of a frequency shift versus mass method averaging over two frequencies was reported to give ≤1.3% accuracy for LO_2, LH_2, and LN_2 for a tilted tank in normal

gravity [4, 10].

A third method investigated in this thesis is radio frequency absorption. This approach is based on the principle that the fluid will absorb energy from an applied electric field and dissipate this energy in the form of heat. This energy dissipation is proportional to the square of the applied electric field. Thus, if illumination of the tank contents is uniform (uniform electric field strength), each parcel of fluid will absorb an identical amount of energy, and dissipation will be directly proportional to fill level regardless of fluid orientation. Absorption methods such as this are generally volume type gauging systems, since the nature of electromagnetic fields permits the wide distribution and detection of energy throughout the tank using a small number of sensors. Antennas or similar structures require only small amounts of space and very little weight.

In summary, future spacecraft designs will require fluid quantity gauging methods which are more accurate than those available presently. These must be capable of measuring cryogenic liquids and remain accurate over long durations. RF gauging methods have advantages over other types, but require uniform electric fields in order for measurement indications to be free from fluid position dependance. Previous attempts at RF gauging have used frequency shift and mode counting to determine fluid volume, however these methods have inherent orientation sensitivity due to the influence of fluid location on resonant electric field structure. Absorption methods have the potential to overcome these limitations.

1.2 Energy Absorption Approaches to Fluid Quantity Gauging

This thesis proposes two electromagnetic absorption approaches to low gravity fluid gauging which address the fluid position dependance of previously investigated RF methods. In the first approach, energy loss in the fluid is determined at a number of resonance frequencies. In the second approach, loss is determined at a frequency far below resonance.

1.2.1 RF Resonance Absorption

RF absorption techniques are based on the principle that dielectric materials absorb energy from applied electric fields and dissipate this energy as heat. This dissipation is proportional to the square of the applied electric field. Thus, if the fields are uniformly distributed throughout the tank, dissipation of energy will be in direct proportion to the volume of fluid, independant of fluid orientation within the tank. However, boundary conditions at the metal tank walls will require electric field at the walls to be zero, as shown in figure 1.1. Field distributions which satisfy these conditions can exist in the tank only for certain frequencies. These are the resonant frequencies of the tank. Electric fields at resonance are non-uniformly distributed in space, and energy loss in the fluid will depend on where the fluid is located within this field distribution. Therefore, loss measurements made at resonance can not be easily related to fluid volume, i.e. volume indication will be sensitive to fluid orientation.

Such orientation dependance can be reduced if loss measurements are made at a number of different resonant frequencies. Figure 1.2 shows three resonant modes in a simple tank structure. Each mode has a unique spatial distribution. With electric field maxima and minima in different locations for each mode, position dependance is also different for each mode. Thus, if the measurements from a number of modes are combined, these errors will be reduced.

Dissipation of energy will be inferred from measurements of quality factor Q. This quantity is the ratio of energy stored to the energy dissipated in the tank-fluid system. Q is easily measured by standard techniques, and can be related to fluid volume if the electrical properties of the fluids are known.

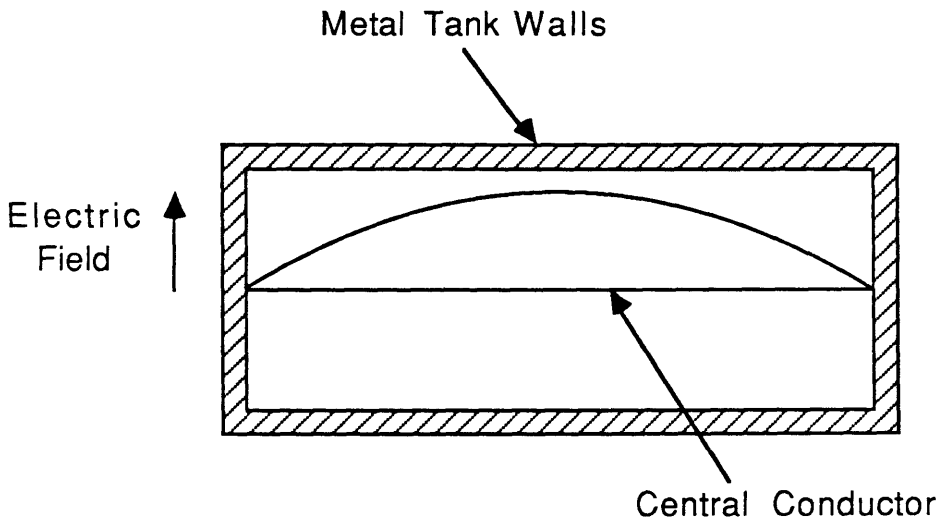

Figure 1.1 The Effect of Boundary Conditions on Electric Field Distribution in a Simple Metal Tank

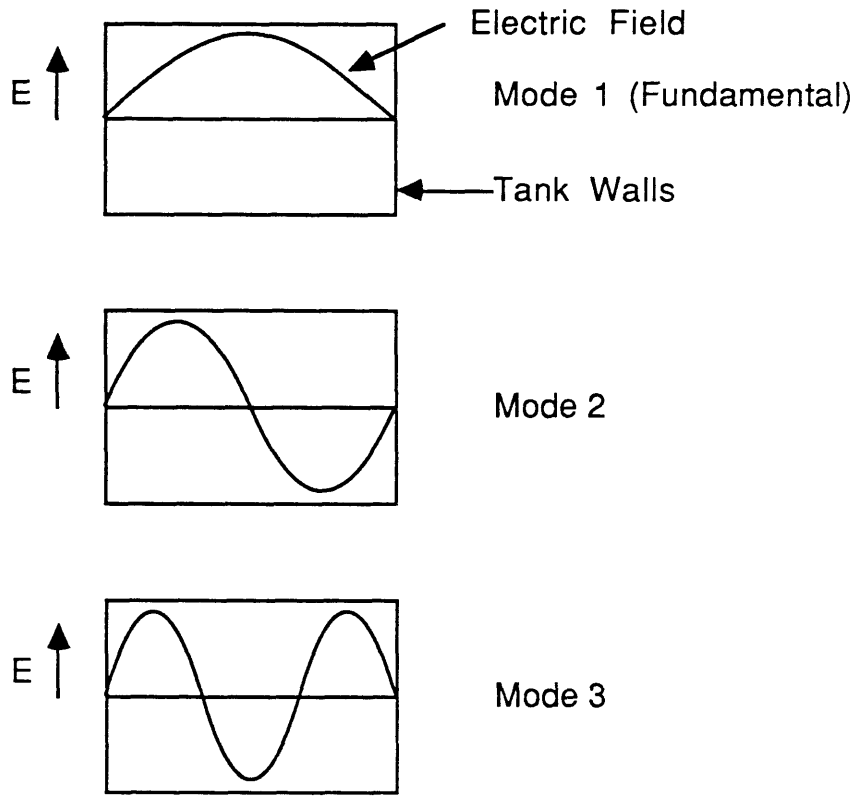

Figure 1.2 Resonant Electric Field Distributions

1.2.2 Non-Resonance Absorption

At frequencies far below the fundamental (lowest) resonant frequency of the tank, the electric field can be made very nearly uniform. Thus, energy dissipation will be more directly proportional to fluid volume than at a single resonant frequency. Quality factor can be measured, and used to relate dissipation to fluid volume, as in resonance methods.

Interaction of the fluid with electric field structure could destroy the field uniformity, however such interaction depends on the real part of the dielectric constant of the fluid. This parameter is defined in section 2.1. For liquid oxygen and liquid hydrogen, dielectric constants are low (1.51 and 1.23, respectively), indicating that the impact on electric field structure will be minimal. Loss measurements in these liquids should therefore give an accurate indication of fluid volume.

Chapter 2

Theoretical Basis For Electromagnetic Absorption Methods Of Fluid Quantity Gauging

2.1 Electromagnetic Absorption Techniques

Electromagnetic absorption approaches to fluid quantity determination in low gravity require measurement of the energy dissipated by the fluid. This energy loss can be related to fluid volume through the quality factor Q of the tank-fluid combination. Q varies inversly with dissipation, and can be easily measured by standard techniques. The Q of any system is defined as

$$Q = \frac{\text{time average energy stored}}{\text{time average energy dissipated}}$$

If the fluid in the tank is considered a dielectric, then its behavior in an electric field can be characterized by the complex permittivity $\varepsilon = \varepsilon' - j\varepsilon''$. This quantity is usually considered a constant for any dielectric. The permittivity of vacuum is often used as a reference, and has the value $\varepsilon_0 = 8.85 \times 10^{-12}$ Farads/meter. The material is then described with the dielectric constant, or relative complex permittivity κ, where

$\kappa = \varepsilon/\varepsilon_0 = \kappa' - j\kappa''$ = dielectric constant
$\kappa' = \varepsilon'/\varepsilon_0$ = real part (energy storage term)
$\kappa'' = \varepsilon''/\varepsilon_0$ = imaginary part or loss factor (dissipation term)
$\tan\delta = \varepsilon''/\varepsilon' = \kappa''/\kappa'$

The quantity $\tan\delta$, defined as the ratio $\varepsilon''/\varepsilon'$, is called the loss tangent, and is commonly used to describe dielectric behavior.

The time average energy stored in a dielectric $\varepsilon = \varepsilon' - j\varepsilon''$ of volume V can be expressed as a funtion of ε',

$$W_s = \frac{1}{2}\int_V \varepsilon' |E|^2 \, dV$$

where E is the electric field inside V.

The time average energy dissipated inside the dielectric has a similar form, related to the loss factor ε",

$$W_d = \frac{1}{2}\int_V \varepsilon'' |E|^2 \, dV$$

As an illustration of relating quality factor to fluid volume in a tank, an ideal tank partially filled with an ideal fluid will be considered. An ideal tank has no energy storage or dissipation in the walls, and the electric field within it is uniformly distributed. An ideal fluid has $\kappa' = 1$ ($\varepsilon' = \varepsilon_0$) with a non-zero loss factor. κ' of the vapor is also 1, thus the electric field in the fluid has the same magnitude as the field in the vapor. In addition, the vapor does not dissipate energy. In this situation, ε' is uniform over the tank volume and ε" is not. Let

V_{vap} = vapor volume
V_{fl} = fluid volume
E = electric field magnitude
ε''_{vap} = loss factor of vapor = 0
ε''_{fl} = loss factor of fluid

Then, the integrals above can be separated into vapor terms and fluid terms,

$$W_s = \frac{1}{2}\int_{V_{vap}} \varepsilon' E^2 \, dV + \frac{1}{2}\int_{V_{fl}} \varepsilon' E^2 \, dV = \frac{1}{2}\varepsilon' E^2 (V_{vap} + V_{fl})$$

$$W_d = \frac{1}{2}\int_{V_{vap}} \varepsilon''_{vap} E^2 \, dV + \frac{1}{2}\int_{V_{fl}} \varepsilon''_{fl} E^2 \, dV = \frac{1}{2}\varepsilon''_{fl} E^2 V_{fl}$$

Since the vapor volume is the difference between tank volume and fluid volume, or

$$V_{vap} = V_{tank} - V_{fl}$$

then the quality factor is

$$Q = \frac{W_s}{W_d} = \frac{\varepsilon' E^2 V_{tank}}{\varepsilon''_{fl} E^2 V_{fl}} = \frac{\varepsilon' V_{tank}}{\varepsilon''_{fl} V_{fl}} = (\text{Constant}) \frac{1}{V_{fl}}$$

Thus, for the ideal tank-fluid combination, Q will vary inversly with fluid volume.

In real systems, the real part of the fluid dielectric constant will not be 1. Although liquid oxygen and liquid hydrogen have low dielectric constants, accurate gauging of these fluids will probably require consideration of the change in energy storage with fluid level due to non-ideal dielectric constant. Dissipation in the vapor and storage in the tank walls will generally be negligible. Let

$W_{s,v}$ = energy stored in vapor
$W_{s,fl}$ = energy stored in fluid
$W_{d,w}$ = energy dissipated in tank walls
$W_{d,fl}$ = energy dissipated in fluid.

The measured Q will then be

$$Q = \frac{W_{s,v} + W_{s,fl}}{W_{d,w} + W_{d,fl}}$$

When the tank is empty,

$$Q_{emt} = \frac{W_{s,v}}{W_{d,w}}$$

where $W_{s,v}$ is evaluated with the tank empty.

To relate Q to fluid volume in non-ideal systems, the storage and dissipation terms are evaluated separately. If the field is uniform, $W_{d,fl}$ will be directly proportional to the fill level. The uniform field assumption allows simplification of the integral expressions for stored and dissipated energy in the fluid as follows:

$$W_{s,fl} = \frac{1}{2} \varepsilon'_{fl} E_{fl}^2 V_{fl}$$

$$W_{d,fl} = \frac{1}{2} \varepsilon''_{fl} E_{fl}^2 V_{fl}$$

where ε'_{fl} = real part of fluid dielectric constant
ε''_{fl} = fluid loss factor
E_{fl} = electric field magnitude in fluid
V_{fl} = fluid volume.

Energy stored in the vapor can be expressed as

$$W_{s,v} = \frac{1}{2} \varepsilon'_v E_v^2 (V_{tank} - V_{fl})$$

where ε'_v = real part of vapor dielectric constant
E_v = electric field magnitude in vapor
V_{tank} = full tank volume

Finally, the energy dissipated in the tank walls is expressed by recalling that $W_{d,w}$ and $W_{s,v}$ together determine Q_{emt}, or

$$W_{d,w} = \frac{W_{s,v} \text{ (evaluated with } V_{fl} = 0)}{Q_{emt}} = \frac{\frac{1}{2} \varepsilon'_v E_v^2 V_{tank}}{Q_{emt}}$$

If these expressions are substituted into the expression for Q, the result is

$$Q = \frac{\varepsilon'_v E_v^2 (V_{tank} - V_{fl}) + \varepsilon'_{fl} E_{fl}^2 V_{fl}}{\varepsilon'_v E_v^2 V_{tank} / Q_{emt} + \varepsilon''_{fl} E_{fl}^2 V_{fl}}$$

For most vapors, $\varepsilon'_v \approx \varepsilon_0$. For uniform fields this permits $E_v \approx \kappa'_{fl} E_{fl}$. Using these approximations and the definitions for dielectric constant and loss tangent, solving for V_{fl} yields

$$V_{fl} = \frac{\kappa'_{fl} V_{tank} (1/Q - 1/Q_{emt})}{\tan\delta + (\kappa'_{fl} - 1)/Q}$$

The ratio of fluid volume to full tank volume is the fractional fill F. Use of F allows easier comparison of the results from different methods. Thus,

$$F \equiv \frac{V_{fl}}{V_{tank}} = \frac{\kappa'_{fl} (1/Q - 1/Q_{emt})}{\tan\delta + (\kappa'_{fl} - 1)/Q}$$

If dielectric constant and loss tangent are known accurately for the fluid, only the measured values of Q and Q_{emt} are required to predict fill level. If these electrical properties are not known exactly, they can be determined by calibration of the system using measured values of full tank Q.

There are a variety of different methods available for the measurement of resonant cavity Q, such as resonance width, standing wave shift, and impedance bridge techniques [12, 13].

The derivation above has neglected the electric field non-uniformities due to resonance mode shapes, discussed in section 1.2.1. The averaging of predicted fill level over three or four frequencies is expected to reduce the magnitude of the resulting errors. Figure 2.1 shows conceptually how averaging over a typical set of resonance field distributions improves effective illumination uniformity.

In summary, the dissipation of electrical energy in a fluid will be proportional to the fluid volume, provided the electric field is uniformly distributed in space. Quality factor Q depends on dissipated energy, and can be measured and related to fluid volume. Energy storage and dissipation in the fluid, vapor, and tank walls must be taken into account in such a derivation. An expression for the predicted fractional fill level F of the tank was derived as a function of Q, measured with the tank empty and at unknown fill levels. F is independant of frequency, thus it can be used in both resonant and non-resonant absorption methods of low gravity fluid gauging.

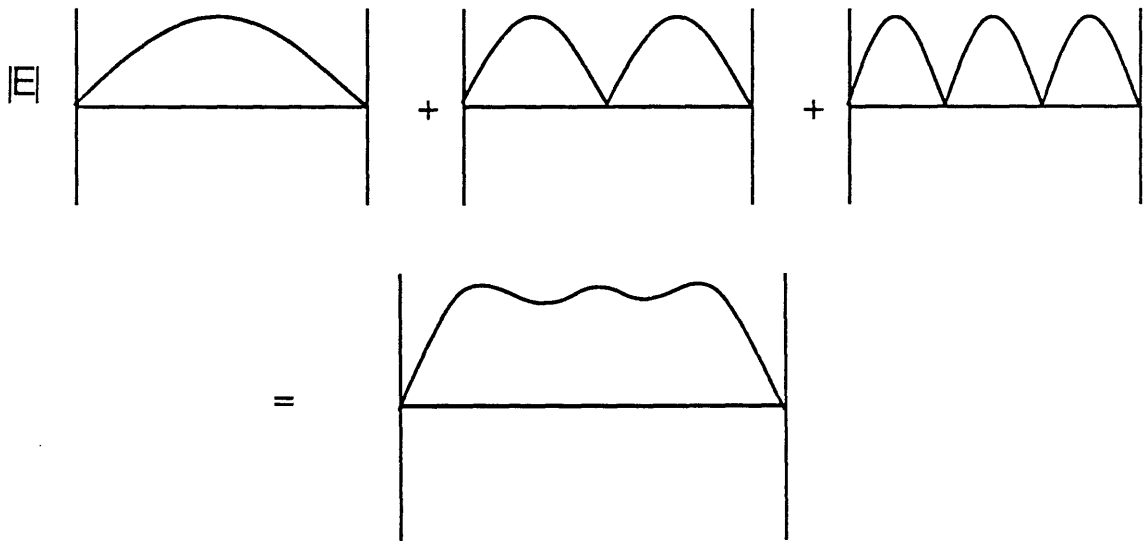

Figure 2.1 Mode Averaging Concept

2.2 Field Non-Uniformities in Electromagnetic Fluid Quantity Gauging

In this section it will be shown that non-uniformities in electric fields will influence accuracy in fluid quantity determinations made from energy dissipation measurements.

This thesis will employ approaches which use frequencies far below resonance, in addition to investigating a resonance averaging technique. Thus the behavior of electromagnetic fields at resonance and in the quasi-static (slowly varying with time) regime will both be considered. This distinction between resonant and quasi-static behavior reflects the fact that EM fields which vary with time are travelling waves with dynamically coupled electric and magnetic fields. Those which have long wavelengths compared to the test tank may be approximated as static fields, for which the electric and magnetic fields are decoupled and there is no wave propagation. As in most RF approaches, it is assumed that the effects of magnetic field interaction with the fluid are minimal.

2.2.1 Electric Fields at Resonance

In the radio frequency gauging methods investigated previously, EM fields propagated through the test tanks as waves. Boundary conditions at the tank walls caused these waves to be reflected, establishing standing waves in the tank. This effect in one dimension is shown in figure 2.2, for a typical tank of length L.

Only those electromagnetic waves which have half-wavelengths which are integer multiples of the tank length L can exist in the tank. When standing wave patterns at these wavelengths exist in the tank, the tank is said to be in resonance. The resonant frequency of the tank depends on the resonant wavelength and the speed of propagation of the waves. Since the wave will travel more slowly through a dielectric than through vacuum, the resonant frequency will be lower when there is fluid in the tank, and will depend on fluid orientation. For fluids with low dielectric constant, such as liquid oxygen and liquid hydrogen, propagation speed is very close to the speed of light in vacuum, and such orientation dependance will be small. For comparison, the dielectric constants are 1.51 and 1.23 for liquid oxygen and liquid hydrogen, respectively. The dielectric constant of vacuum is 1.

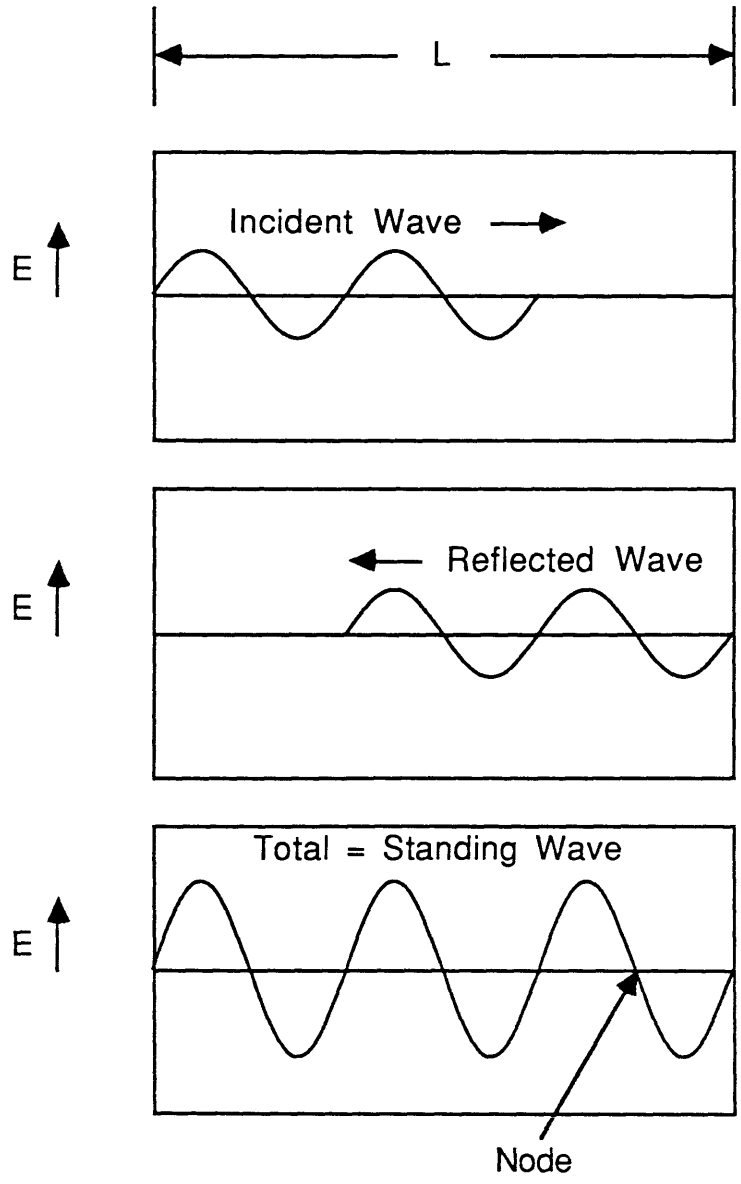

Figure 2.2 Standing Wave in One Dimension

If waves of a broad range of frequencies are supplied to the tank using the circuit shown in figure 2.3, only energy at or very near the resonant frequency will be absorbed by the tank. These resonances appear as loss maxima at the detector, with center frequencies determined by the resonance wavelengths and the speed of propagation in the tank. Fluid quantity gauging techniques which depend on Q measurement are often termed 'resonance width techniques', as the Q is related to the shape of this curve according to

$$Q = \frac{f_0}{\Gamma}$$

where f_0 is the resonance frequency, and Γ is the resonance width at half maximum.

The electric fields which exist at resonance are termed the resonance modes, and for the tank in figure 2.2 they have a longitudinal spatial distribution which goes as

$$E(x) = 2E_0 \cos\omega t \sin\left(\frac{n\pi x}{L}\right)$$

where ω = angular frequency of the source

n = mode number or index

E_0 = amplitude of original incident wave

This field distibution is not uniform in space. In terms of fluid gauging, loss due to absorption of energy by the fluid will depend on where the fluid is located in the tank, as the electric field strength varies from place to place along the tank length. For example, a parcel of fluid placed in an electric field maximum will induce a larger change in Q than one placed in a resonance node. This results from the direct dependance of energy dissipation on electric field strength, as discussed in section 2.1. If Q is measured at a number of resonant frequencies, this orientation dependance should be reduced, since the spatial distribution at each frequency is unique.

In real tanks, and in the presence of fluid, the solution to the boundary value problem above becomes difficult to obtain. Baffles, aquisition devices, and less than ideal tank geometries can force very complicated resonant field distributions. The resonant frequency will depend on internal tank structure as well as on fluid volume, dielectric constant, and orientation. However, the mode averaging concept described above should still reduce the dependance of volume determination on fluid position, since it depends on dissipated energy and not on resonant frequency.

In summary, reflection of incident waves at tank walls will cause standing waves (resonances) in both the fluid and vapor. The wavelengths of these standing

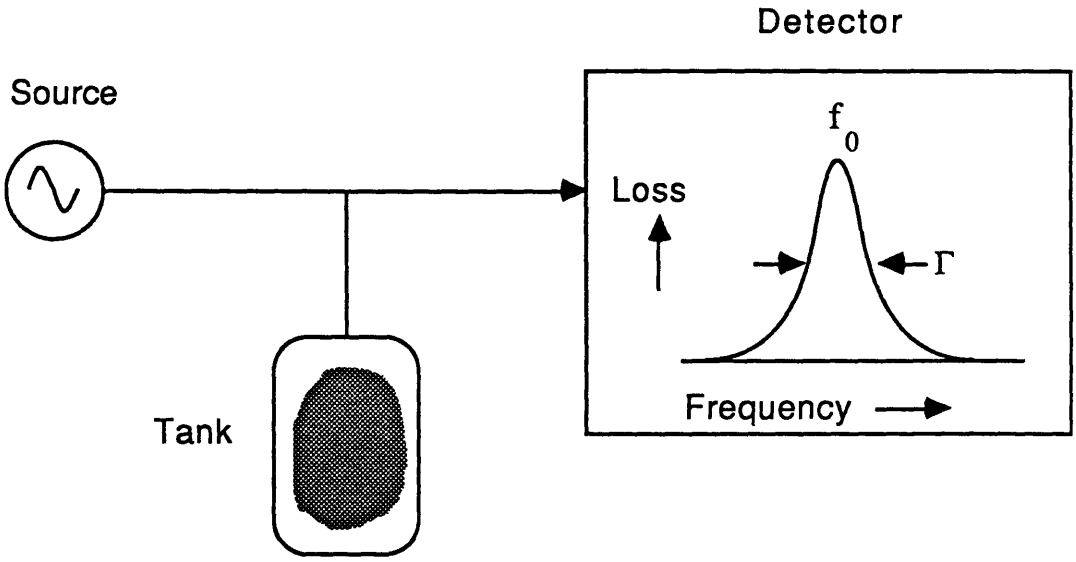

Figure 2.3 Simple Resonance Detection Circuit

waves will be determined by boundary conditions at the tank walls and the electrical properties of the fluid. The non-uniform electric field distribution of these resonance modes will cause orientation dependance of fluid quantity determinations based on loss measurements made at a single frequency. However averaging the results of loss measurements made at a number of resonant frequencies should reduce this dependance. The small dielectric constant of LO_2 and LH_2 minimizes the adverse effects of fluid-field interaction at resonance.

2.2.2 Fluid Interaction with Static Electric Fields

If a uniform static electric field is established in vacuum and a dielectric slab placed inside it, as shown in figure 2.4, the field will maintain its uniformity in space but will be reduced in magnitude inside the slab. If the electric field strength in vacuum is E_o , then the field in the dielectric slab will be E_o/κ', where κ' is the dielectric constant of the slab. The field will have the same strength whether the slab is oriented parallel or perpendicular to the original field.

Fluids in low gravity can not be expected to have simple configurations such as this. The absence of gravity or other accelerations causes capillary forces to minimize the surface area. This subject is discussed in more detail in Appendix B. The result is that the liquid vapor interface will in general be a curved surface. A typical configuration is shown in figure 2.5. Note that bubbles might also be present. In such a situation, boundary conditions at the interfaces will distort the electric field.

As an example, a uniform field can be established in an ideal parallel plate capacitor as shown in figure 2.6. The figure represents the cross section of a square tank. With a typical low-g liquid vapor interface between the plates, boundary conditions at the plates and at the interface will result in an electric field like that shown in figure 2.7. Far enough from the surface, the field strength will be $\kappa' E_o$, as in the ideal case. However, close to the surface the field lines will bunch together, creating a larger field strength. If $\kappa' \approx 1$ then the field in the fluid will be almost identical to the field in the vapor. Refraction of the field lines at the interface also depends on κ', thus bending of the field lines will also be negligible when $\kappa' \approx 1$. It is also clear that with any fluid, surface curvature should be small to minimize field distortions.

Fringe effects normally neglected in discussions of electric fields in parallel plate or similar structures will also depend on surface shape and dielectric constant. For a dielectric slab between two parallel plates, such effects might appear as in figure 2.8.

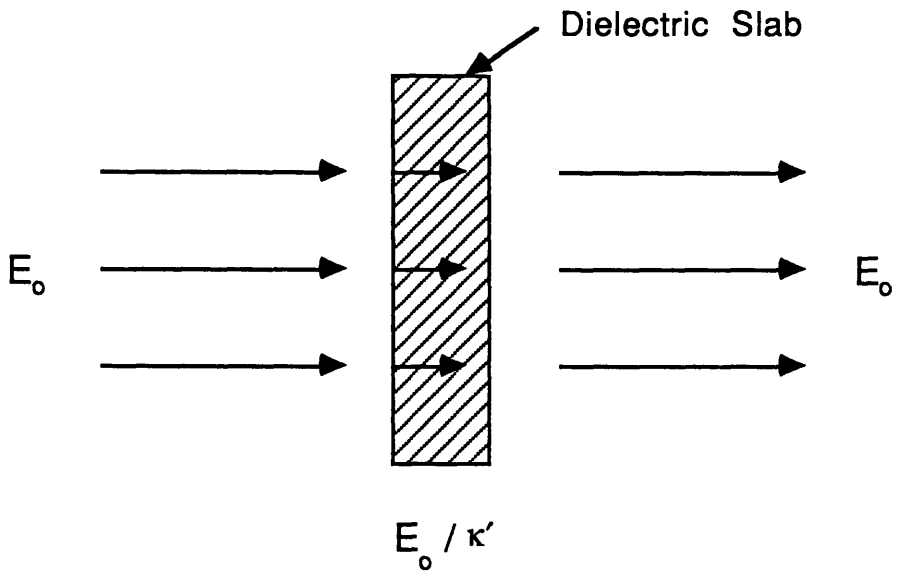

Figure 2.4 Dielectric Slab in a Uniform Electric Field

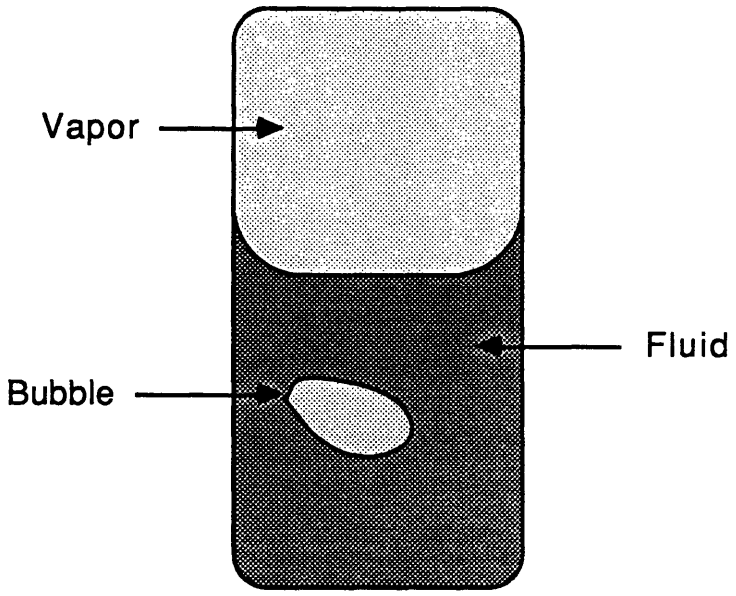

Figure 2.5 Typical Low-g Fluid Configuration

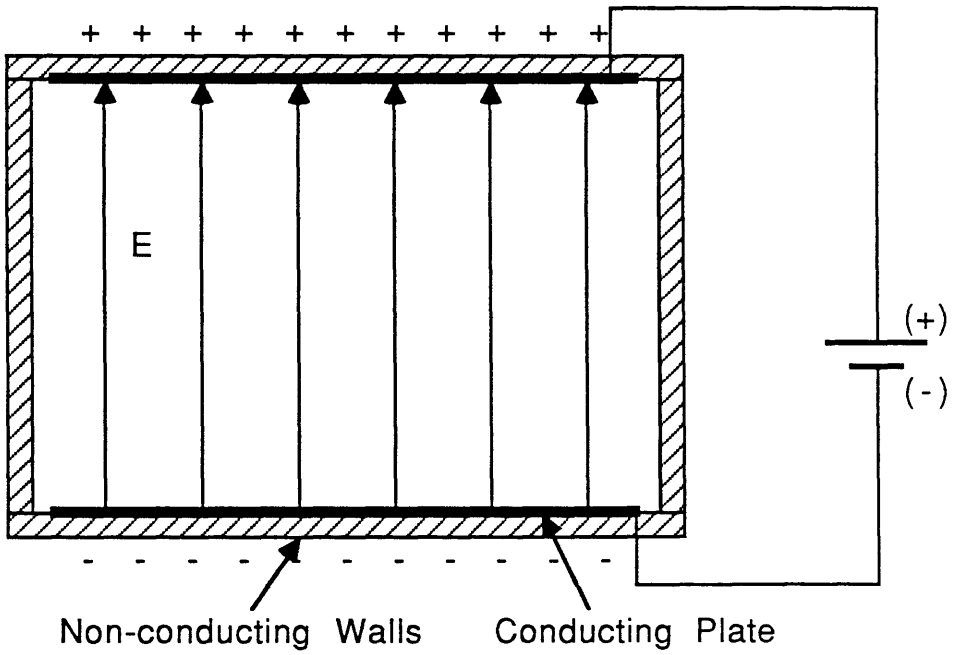

Figure 2.6 Uniform Electric Field in a Parallel Plate Capacitor

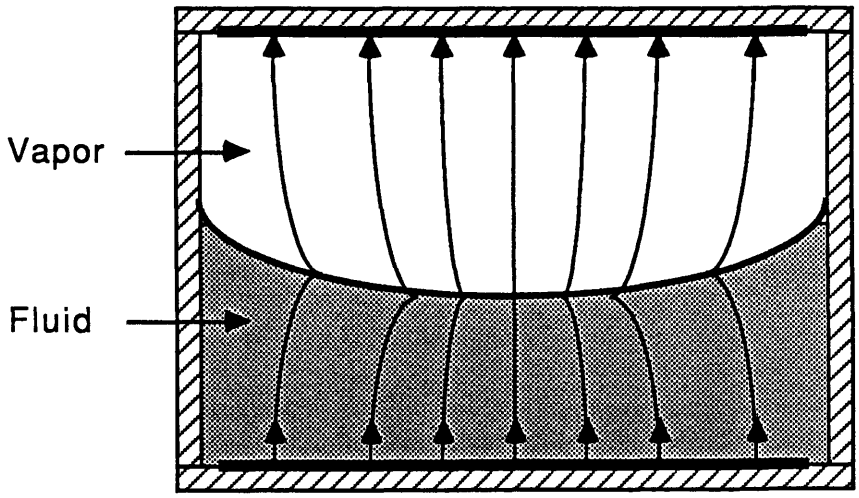

Figure 2.7 Electric Field Distortion in a Typical Fluid Configuration

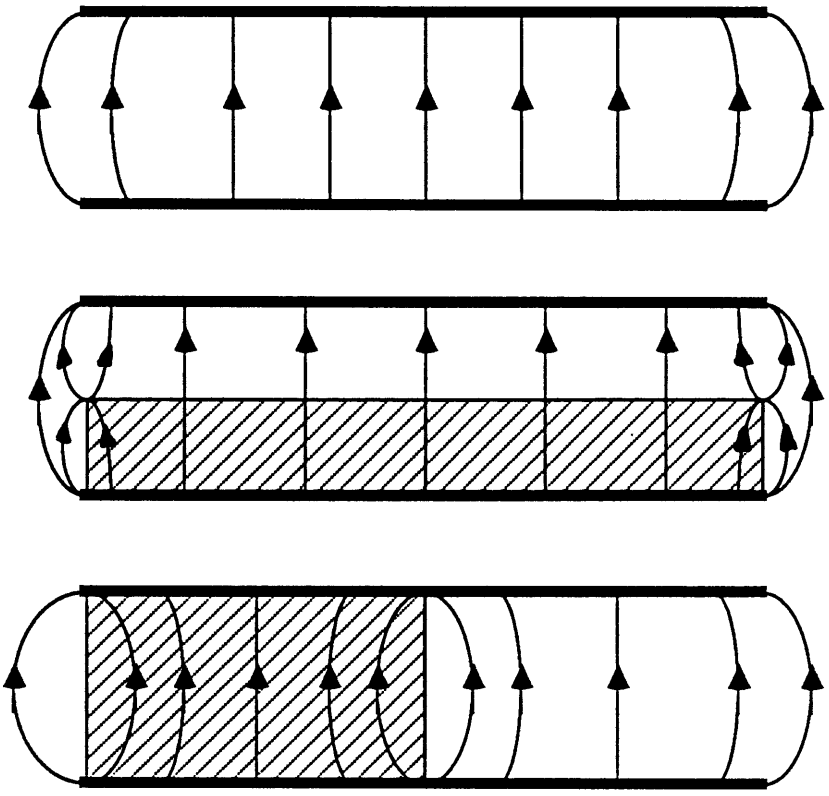

Figure 2.8 Fringe Effects in a Partially Filled Parallel Plate Capacitor

The spacing or bunching of field lines will in general have an impact on energy storage and dissipation in the fields, and thus can have impact on the accuracy of energy absorption gauging methods.

In the case where a droplet of fluid is floating free in the vapor, the uniformity of the applied field is distorted as shown if figure 2.9. The field in the fluid can be shown to be [11]

$$E_{fluid} = \frac{3\kappa'_1}{\kappa'_2 + 2\kappa'_1} E_0$$

where E_0 is the originally uniform applied field and κ'_1 is the dielectric constant of the vapor, which can be assumed to be 1. This will cause the field in the fluid to be less than it would be if the fluid was in the simple configurations shown earlier, especially with large κ'. Low values of dielectric constant will minimize such distortions. For example, the electric field within spheres of liquid oxygen and liquid hydrogen would be

$$E_{LO_2} = 0.855E_0$$

$$E_{LH_2} = 0.929E_0$$

Note that the 15% reduction of the field strength in liquid oxygen would cause only a small error in fluid volume prediction, because in low gravity only a small percentage of fluid is expected to be in such spheres (see Appendix B). The electric field within the remainder of fluid (away from curved surfaces) is uniform, and is determined only by the dielectric constant, according to $E = E_0/\kappa'$.

For the case where an ullage bubble is floating in liquid, $\kappa'_2 = 1$ and the field inside the bubble is stronger than the field in the surrounding fluid by the factors 1.170 and 1.076 respectively.

In summary, Q measurements depend on energy storage and loss in the fluid-tank system, and can be related to fluid volume. Q is easily measured, however accuracy in fill volume determination depends on electric field uniformity. Liquid-vapor interface shape and boundary conditions determine electric field uniformity in static (or quasi-static) situations. The low dielectric constants of LO_2 and LH_2 will

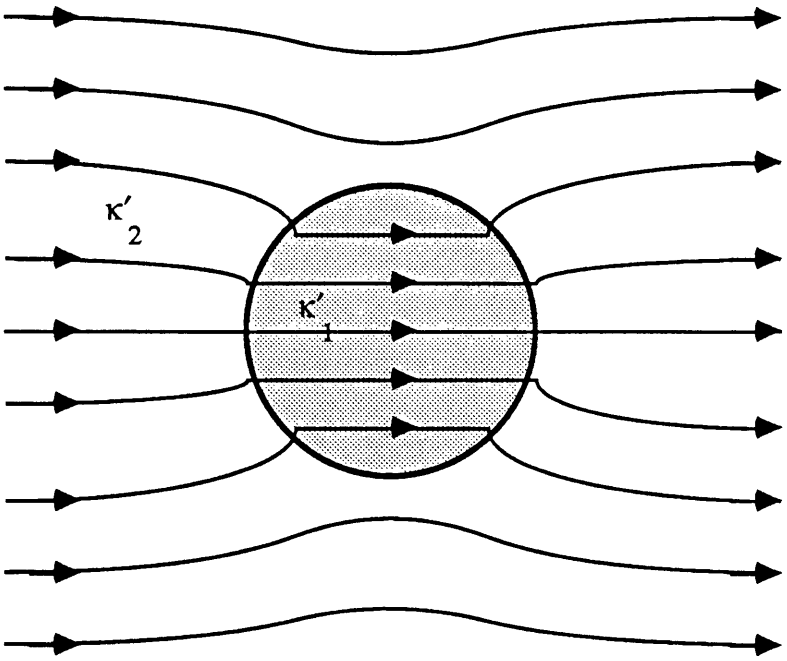

Figure 2.9 Dielectric Sphere in Uniform Applied Field

keep non-uniformities relatively small in cryogenic tanks, and therefore low frequency Q measurements of these liquids should have good accuracy even in low gravity.

Chapter 3

Experimental Description

3.1 RF Resonance Absorption Experiment

In this experiment, absorption of energy by the fluid was inferred from measurements of the quality factor of the tank-fluid system at a number of resonant frequencies. Normalized fractional fill was calculated from the Q measurements using the expressions derived in section 2.1. The results at each frequency were averaged to reduce position dependance due to the resonance mode field distributions discussed above.

Measurements were made with two fluids having substantially different loss tangents. A low loss tangent fluid was used to simulate liquid hydrogen and liquid oxygen over the full range of tank fill levels. In order to determine the sensitivity of the approach to small changes in fill level, a high loss tangent fluid was used. Although fluids with high loss tangents allow observation of small changes in liquid level, at higher fill levels the resonance peak broadens to an extent that resonance width measurement techniques are not appropriate. The high loss tangent fluid was therefore used only at low fill levels. Two test set-ups were required to accomplish this comparison.

3.1.1 Low Sensitivity Measurement Set-up

Quality factor measurements were taken at three resonant frequencies of a coaxial right circular cylinder, pictured in figure 3.1. The tank was constructed of 3" i.d. copper tubing, with solid copper end plates secured with threaded rod. The central conductor was 1/16" copper rod and was electrically connected at the tank bottom. The structure was fed from a standard N-type connector mounted in the top. The central conductor was electrically connected to the center conductor of this connector. The full

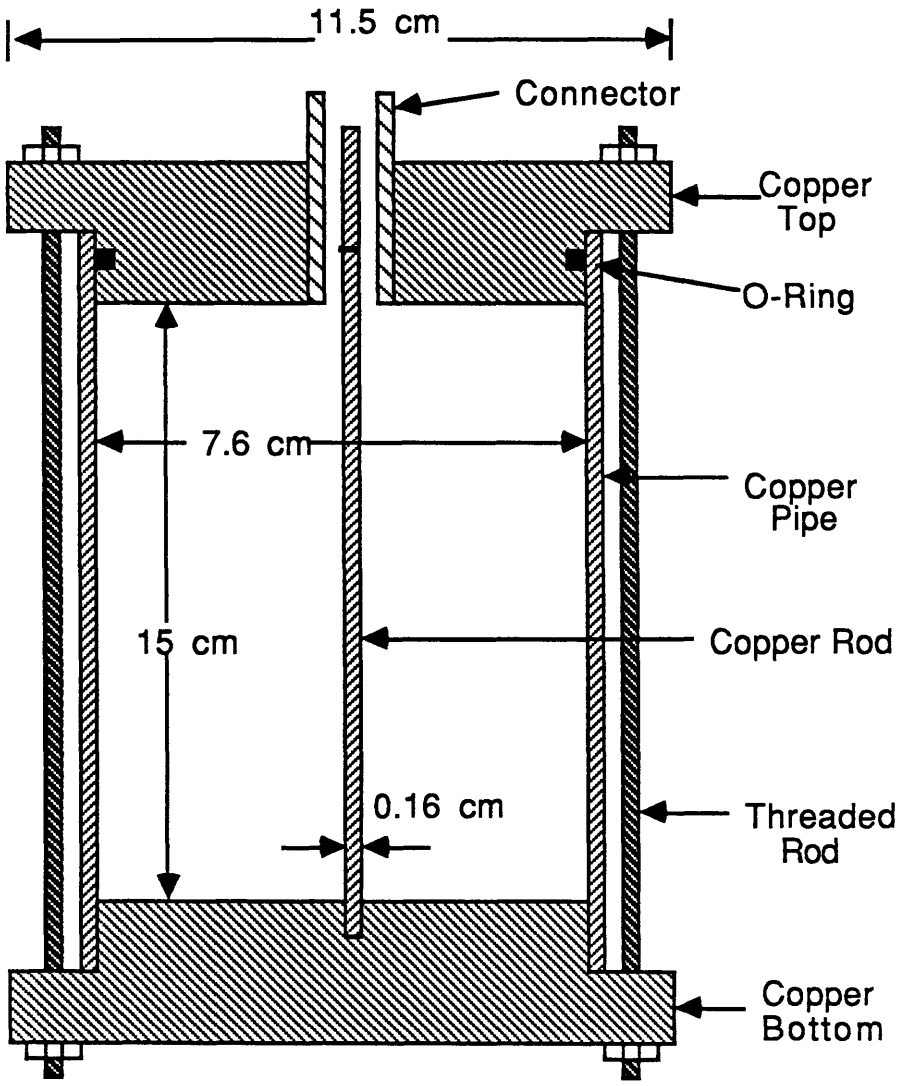

Figure 3.1 Test Tank For Resonance Absorption Experiment

tank volume was 660 ml.

This structure was designed to have a fundamental empty tank resonance (TEM_{100}) at f_0 = 1 GHz. The mode shapes for the fundamental and first two harmonics are shown in figure 3.2. The TEM modes were excited by RF energy supplied through the center conductor.

The measurement set-up is shown schematically in figure 3.3. A sweep oscillator generated a microwave signal which automatically swept frequency over a specified range. Operation at a fixed, manually adjustable frequency was also possible. The signal passed through a coax 'tee' to a crystal detector and oscilliscope. The crystal converted the signal into a voltage which was proportional to the power in the signal. When the oscillator was in the automatic sweep mode, visual inspection of the resonance amplitude as a function of frequency was possible. The tank was connected to the rest of the circuit through a precision vernier slotted coax device, which had a third crystal detector on a moveable carriage calibrated in centimeters. With the oscillator in the fixed frequency mode, detection of the standing wave maxima and minima in the slotted coax was possible. Frequency measurements were taken from the sweep oscillator scale markings, which were calibrated to a commercial wavemeter, and were accurate to within ± 0.2%.

The effects of energy dissipation and storage by the external circuit must be removed from measurements of Q in order to determine loss due to the tank alone. The loaded Q (Q_L) is the total Q of the system, and includes the effects of the circuit. The unloaded Q (Q_U) is the Q due solely to the tank and fluid. These two quantities are related by the voltage standing wave ratio (VSWR) measured at resonance in the line feeding the tank, as follows [12],

$$Q_U = (1 + VSWR)\, Q_L$$

Loaded Q was determined at each fill level by varying the frequency above and below each resonance, and observing the shift of standing wave minima in the slotted coax. VSWR at resonance was also measured using the slotted coax, crystal detector, and integrating voltmeter. The procedure is described in detail in reference 12.

Accuracy of Q_U measured by this technique was estimated at ± 15%. This was limited mainly by the graphical nature of a portion of the procedure. Errors in dielectric constant and loss tangent were taken to be negligible compared to this error.

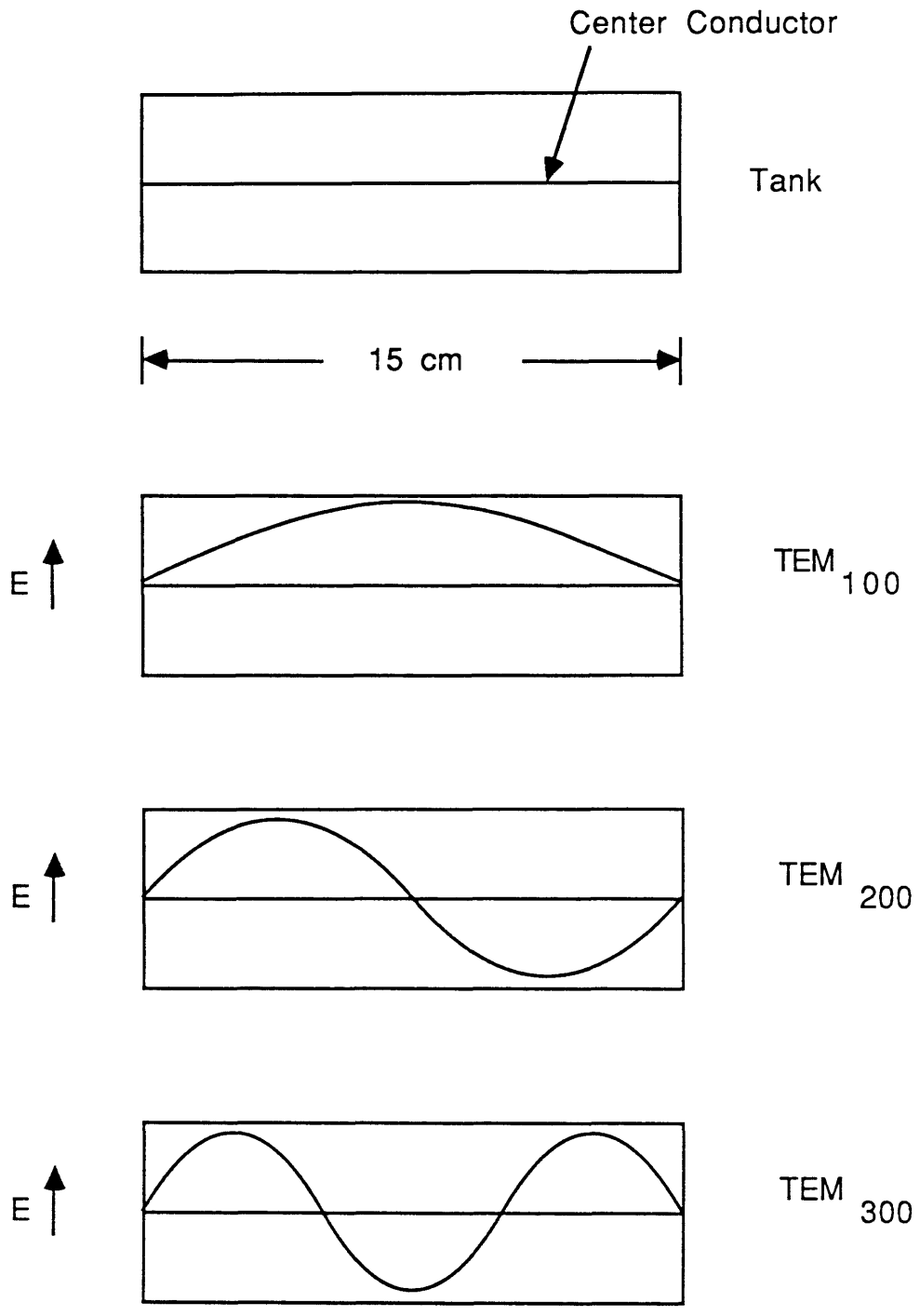

Figure 3.2 TEM Modes in Cylindrical Test Tank

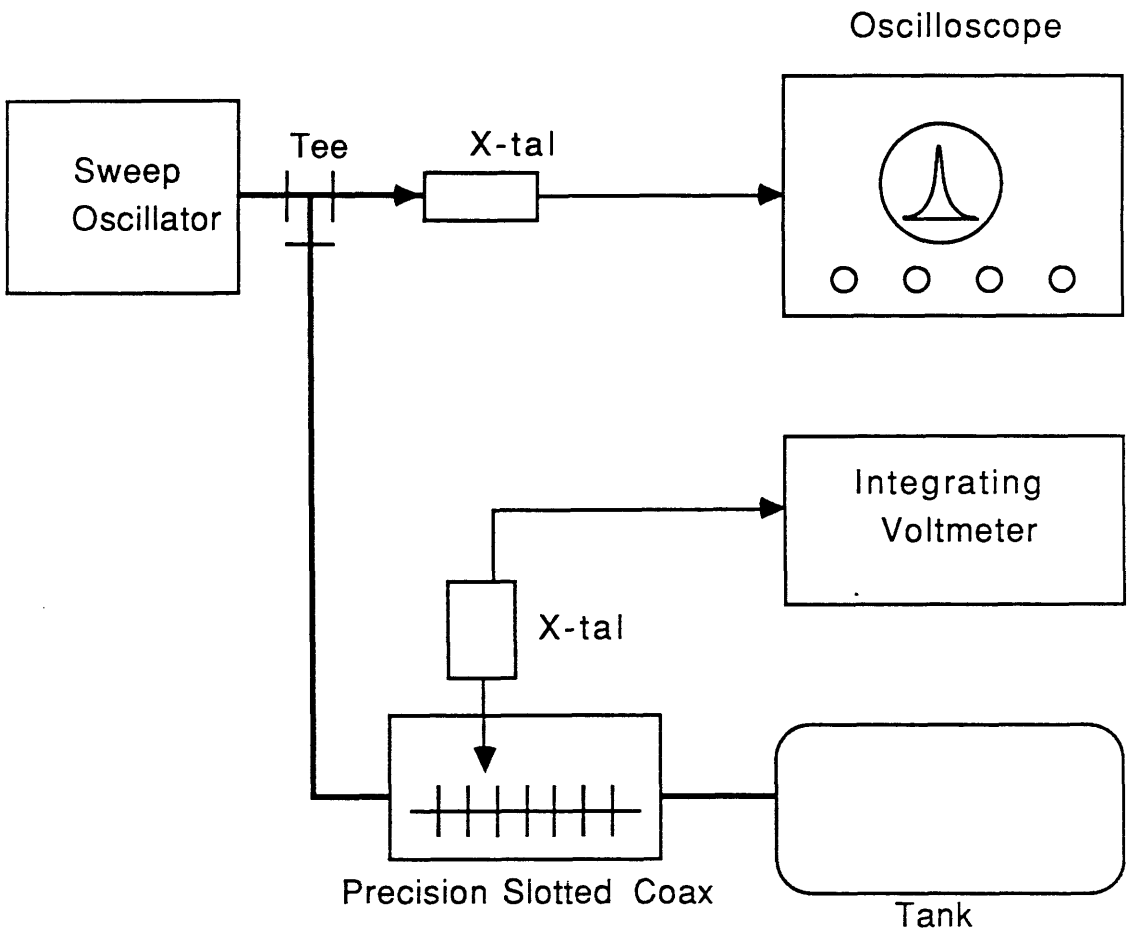

Figure 3.3 Low Sensitivity Measurement Set-up

3.1.2 High Sensitivity Measurement Set-up

The set-up for measurements using the high loss tangent fluid is shown in figure 3.4. In order to detect small changes in fluid level, oscillator output amplitude was required to remain stable. This was accomplished by passing the output through a 3 dB directional coupler, and converting a portion of the signal to a voltage with a crystal detector. This voltage was returned to the oscillator and used to regulate signal amplitude. The signal was then passed by a commercial wavemeter to a waveguide 'tee' and crystal detector. The detector output was observed on the oscilliscope and the resonance amplitude and wavemeter marker were visible as a function of frequency. The tank was coupled to the circuit through a standard slotted coax. This device had a moveable crystal detector with broader frequency range (7 to 12 GHz) than the vernier slotted line used in the low sensitivity measurements. This permitted measurement of Q over four resonance modes. VSWR and standing wave shifts were measured with the slotted coax and crystal detector.

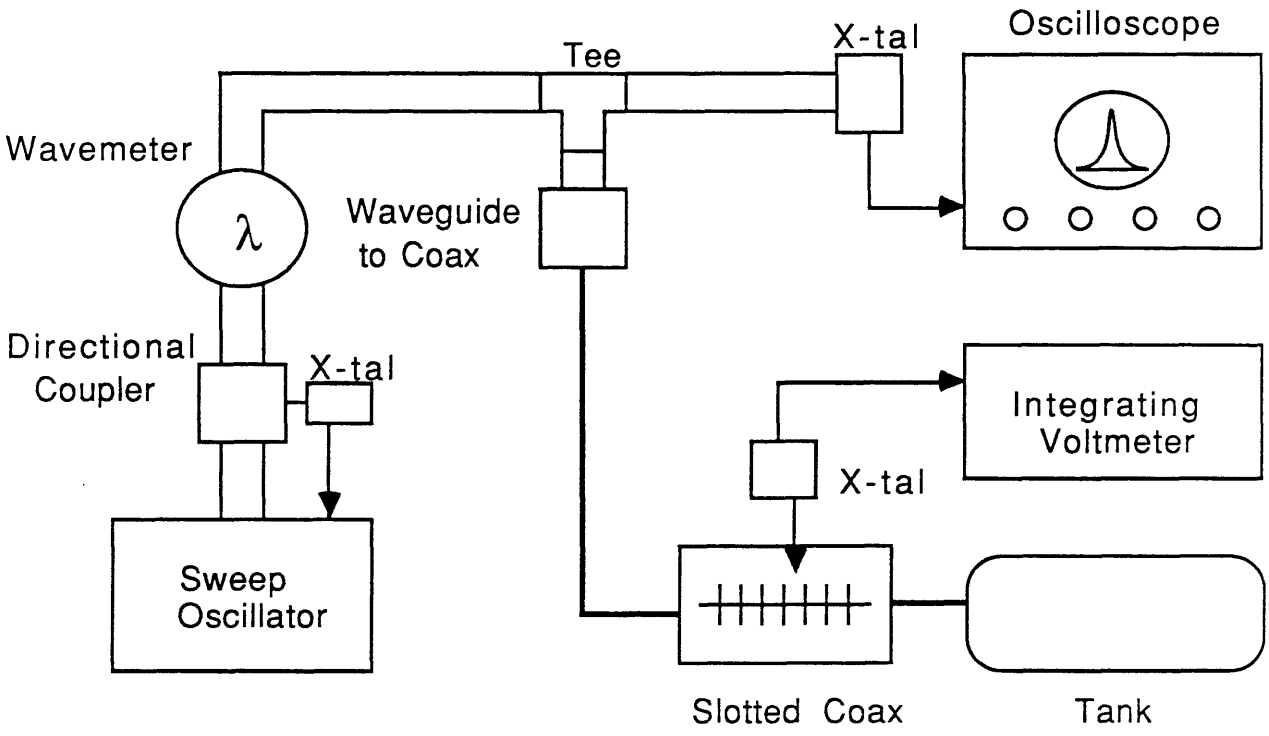

Figure 3.4 High Sensitivity Measurement Set-up

3.2 Non-Resonance Absorption Experiment

In order to study absorption effects in non-resonant electric fields, a tank was configured as a parallel plate capacitor and run well below any electromagnetic resonances. This resulted in a nearly uniform, quasi-static electric field. The tank is shown in figure 3.5, and the electric field structure, neglecting the effects of the acrylic walls, is shown in figure 3.6. The plates were 1/16" copper and were 77 by 76 cm, or 0.585 m^2. Plate spacing was 10 cm. The tank was isolated from external EM sources, in order to minimize field non-uniformities. The full tank volume (volume between the plates) was 58.52 liters.

Measurements were taken with a standard impedance bridge. The set-up used is shown in figure 3.7. Operating frequency of the unit for all measurements was 1 kHz. Plate voltage was a constant 600 mV ± 10 mV (AC). The capacitor plates were connected to the impedance bridge by a short length of coaxial cable, which shielded most of the length of wire to the bridge. The short, unshielded leads were spaced apart to reduce stray capacitance.

The bridge circuit employed by the instrument is shown in figure 3.8. The tank is placed as shown in the circuit and a voltage applied at the top of the bridge. The adjustable resistances (potentiometers) are tuned until the voltmeter in the center of the circuit reads zero ("null"). Q and C are then read from calibrated dials mounted on the appropriate potentiometers, as shown.

Accuracy of the instrument was given by the manufacturer for 1/Q as ± 5% ± 0.001, where ± 0.001 is a fixed accuracy term which is always added to the percentage accuracy term. In the range of Q values found in this experiment, this was equivalent to ± 25% at empty tank, and ± 7.5% at full tank. Capacitance measurements had accuracy of ± 2.5 %. Dielectric constant determination was based on capacitance measurement as described in Appendix C, therefore error in dielectric constant was ± 5%. Loss tangent was determined from empty and full tank Q measurements, and had ± 9% error.

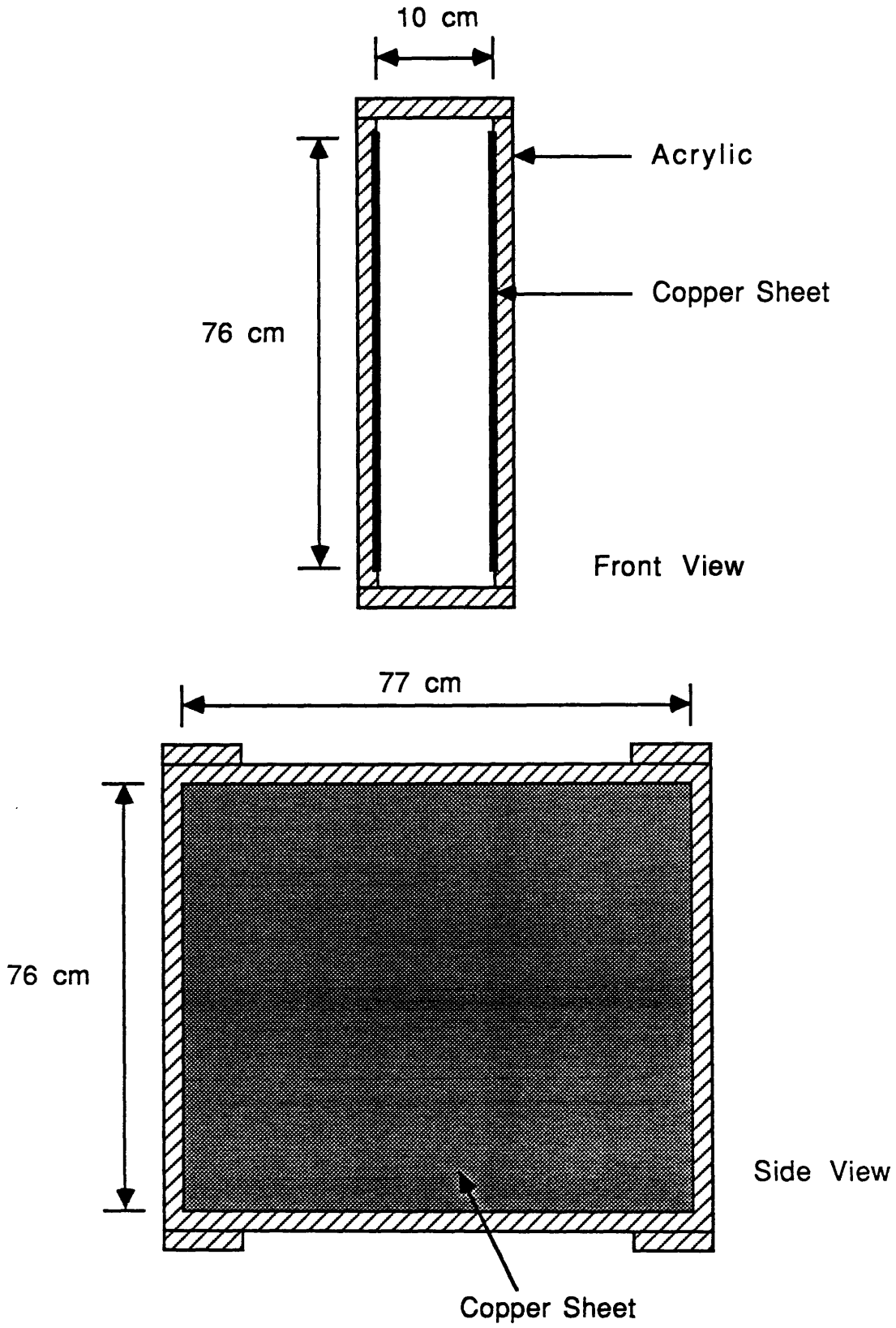

Figure 3.5 Non-Resonance Test Tank

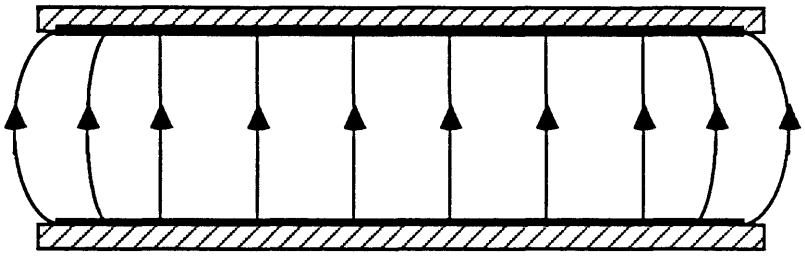

Figure 3.6 Electric Field in Parallel Plate Test Tank

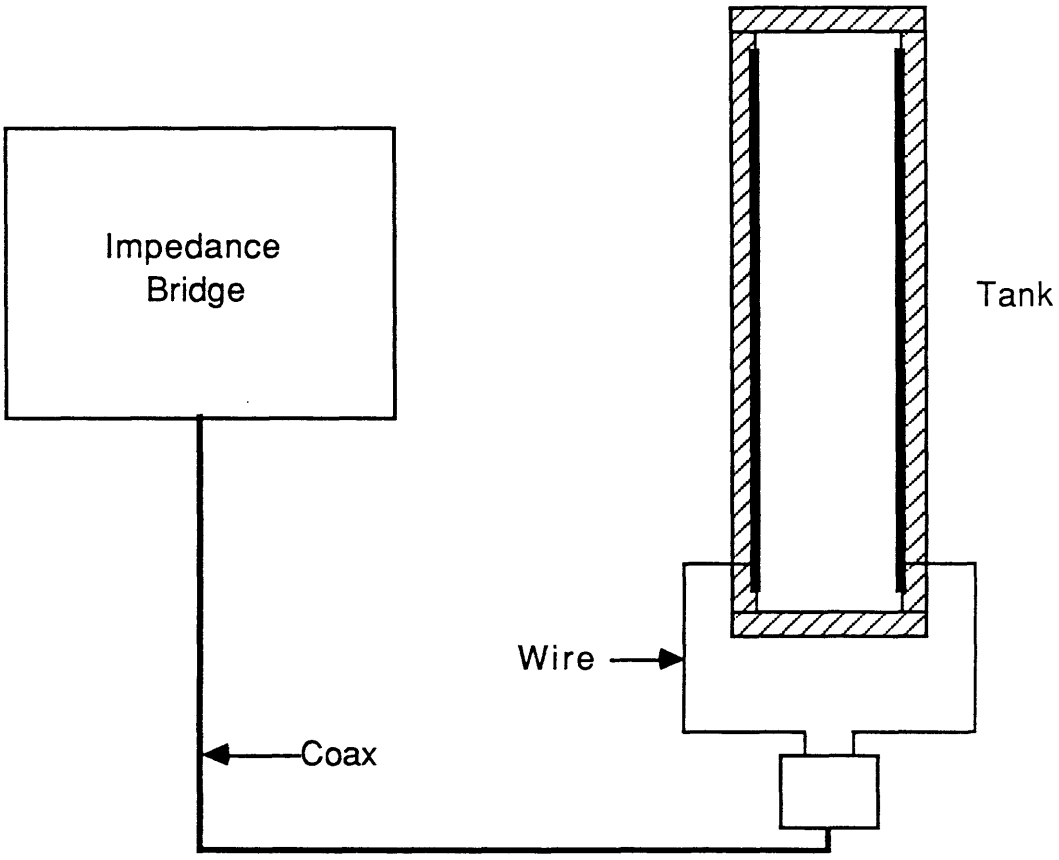

Figure 3.7 Non-Resonance Absorption Measurement Set-up

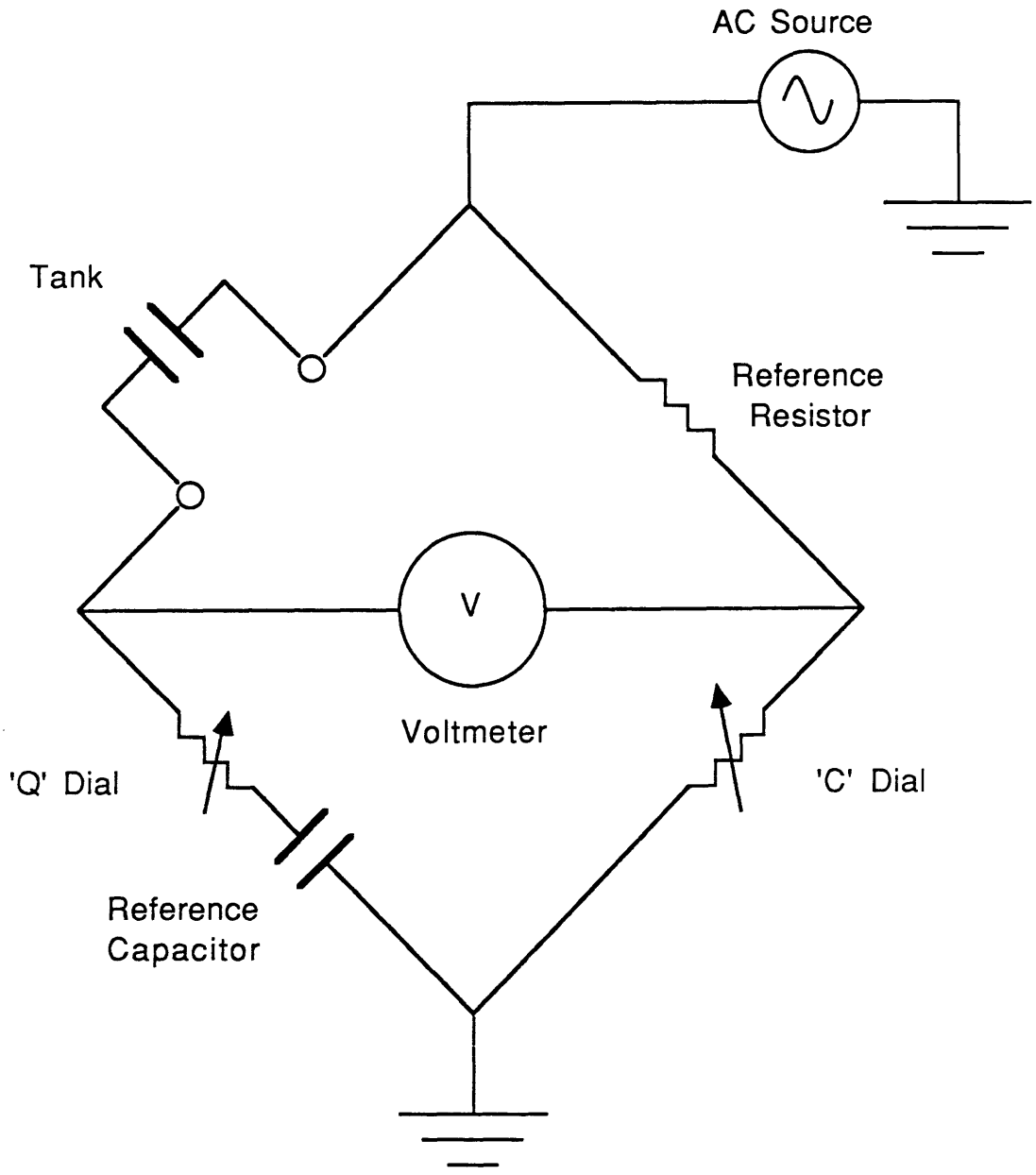

Figure 3.8 Basic Bridge Ciruit For Measuring C and Q

Chapter 4

Experimental Results

4.1 RF Resonance Absorption Experiment

4.1.1 Low Sensitivity Measurements

In the low sensitivity tests, kerosene was used to simulate liquid oxygen and liquid hydrogen, which at 3 GHz have loss tangents of about 10^{-3} and and 10^{-7}, respectively. Loss tangent for kerosene is 0.0045 at 3 GHz. The dielectric constant for kerosene is 2.09 at 3 GHz, which is close to the dielectric constants of liquid oxygen (1.51) and liquid hydrogen (1.23).

Unloaded Q was determined with the tank in the vertical and horizontal orientations shown in figure 4.1, for fill levels of 0, 100, 200, 300, 400, 500, 600, and 660 ml (full tank) at each of three resonant frequencies. Predicted fill volume V_{fl} was calculated using Q_U and the expression for fractional fill derived in section 2.1,

$$F \equiv \frac{V_{fl}}{V_t} = \frac{\kappa'_{fl}(1/Q - 1/Q_{mt})}{\tan\delta + (\kappa'_{fl} - 1)/Q}$$

where $V_t = 660$ ml

$\kappa'_{fl} = 2.09$

$\tan\delta = 0.0045$

The TEM_{n00} modes for n = 7, 8, and 9 were used, and these had the measured empty tank resonance frequencies shown below.

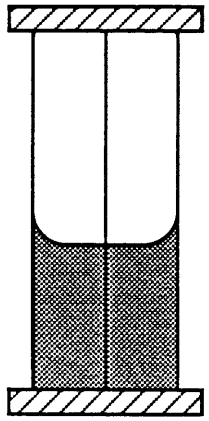

Vertical Orientation

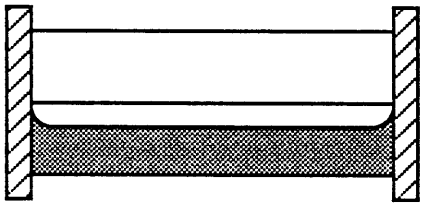

Horizontal Orientation

Figure 4.1 Tank Orientation

mode	frequency
n = 7	7.179 GHz
n = 8	8.132 GHz
n = 9	9.005 GHz

The small variations from the design values of 7, 8, and 9 GHz were attributed to the end connector and imperfect cavity surfaces. The electric field distribution for mode 7 is shown in figure 4.2.

Plots of actual fill level versus predicted fill level V_{fl} are shown in figure 4.3, for modes 7, 8, and 9. For each mode, the vertical and horizontal orientation dependance can be seen as a difference between the vertical and horizontal plots. Substantial error in predicted fill is also visible for both orientations. Much of this is thought to be due to the longitudinal variation in resonant electric field structure, which could account for the apparant oscillatory nature of the plots. As discussed in section 2.2, dissipation is reduced when the fluid is located in regions of reduced electric field. Thus, increases in fluid level occuring near a resonance node will appear as small changes in predicted fill. Similarly, larger changes in predicted fill will occur as fill levels pass through resonance anti-nodes. It is possible that Q measurements taken at smaller increments of fill would have shown this effect in detail. The longitudinal spatial distribution is essentially undersampled for eight fill levels. Thus, the effect will be discussed in more detail for the high sensitivity measurements, where smaller increments of fill level were used.

For each tank orientation, the numerical average of predicted fill values for all three modes was taken, and the results plotted in figure 4.4. Single mode values are plotted as points, while averaged values are connected with lines. The effect of mode averaging in reducing the difference between vertical and horizontal predicted fill can be seen. A reduction of fluid position dependance is seen as a reduction of the difference between vertical and horizontal test results. However, error in predicted fill remains. Much of the error is thought to be due to the radial electric field variation around the central conductor. This field non-uniformity causes predicted fill to increase rapidly as the fluid approaches the central conductor in the horizontal orientation. In the vertical orientation, the radial dependance is added to the longitudinal dependance caused by resonance mode shapes. The longitudinal dependance is reduced by averaging, while the radial dependance is not. There were also errors likely in Q_U for mode 9. This resonance was difficult to track as fill level increased, and the possibility exists that

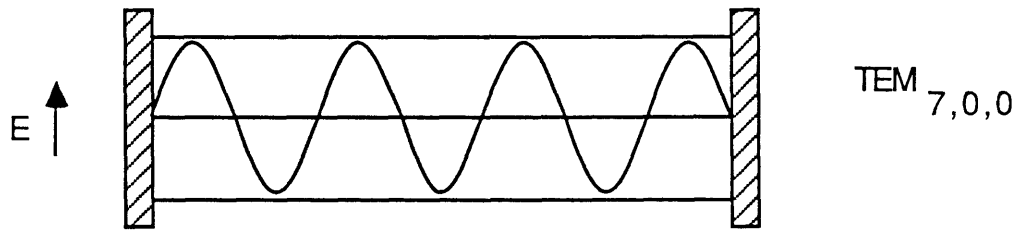

Figure 4.2 Electric Field Resonance Mode Distribution

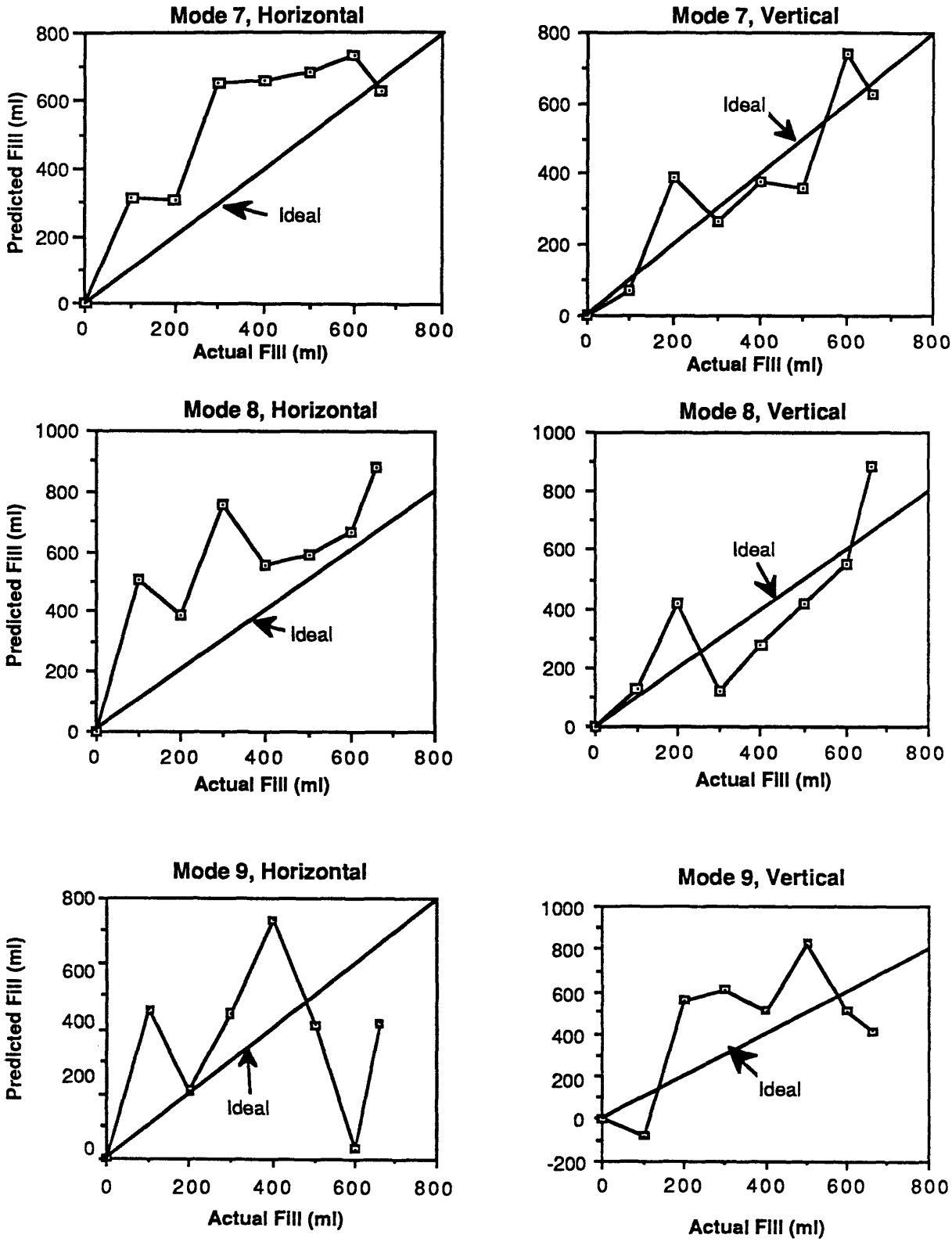

Figure 4.3 Low Sensitivity Experiment Results, Modes 7, 8, & 9

Figure 4.4 Kerosene Mode Averaged Fill Level

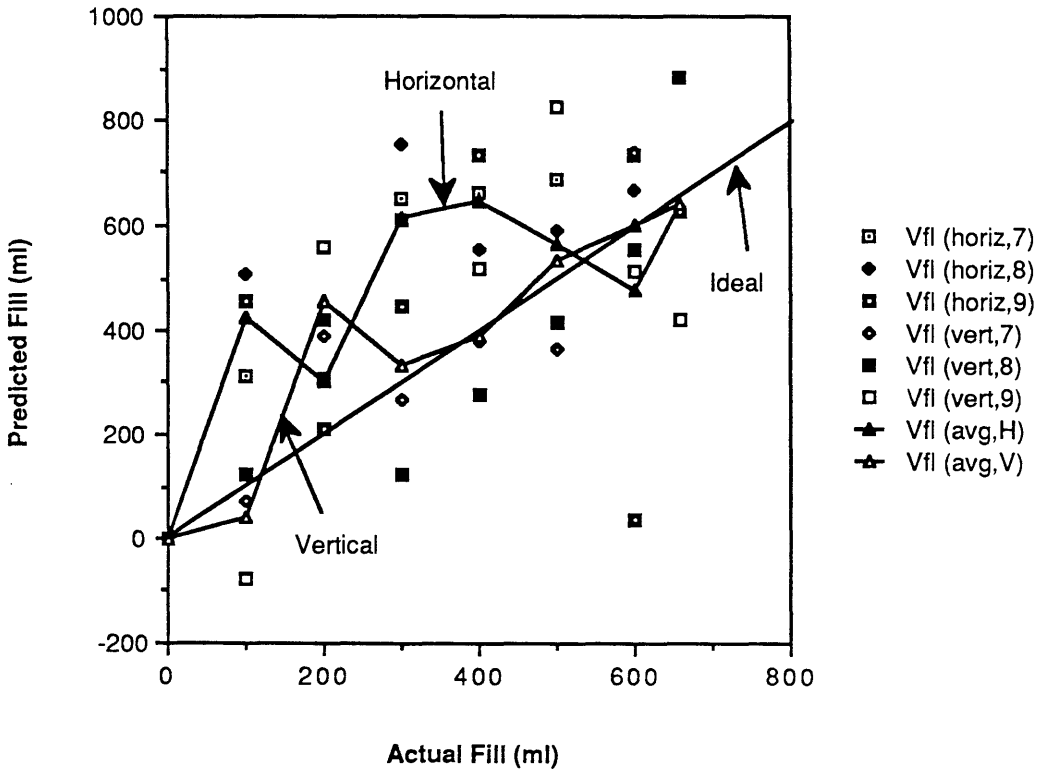

spurious resonances were measured at certain fill levels. This demonstrated the difficulties inherent in resonance detection methods, especially at high frequencies, as discussed in section 2.2.1.

4.1.2 High Sensitivity Measurements

For the high sensitivity measurements, ethyl alcohol was used as the test fluid. Loss tangent for this fluid was high (on the order of 0.6), permitting small changes in fluid level to be observed. Dielectric constant was about 4 at the frequencies used. The dielectric constant and loss tangent varied with frequency, and exact values at the frequencies used are given in Appendix C.

Unloaded Q was determined with the tank in the same vertical and horizontal orientations used in the low sensitivity measurements, for fill levels of 25, 50, and 100 ml at each of four resonant frequencies. Predicted fill level V_{fl} was calculated using Q_U and the expression for fractional fill derived in section 2.1,

$$F \equiv \frac{V_{fl}}{V_t} = \frac{\kappa'_{fl}(1/Q - 1/Q_{mt})}{\tan\delta + (\kappa'_{fl} - 1)/Q}$$

where V_t = 660 ml, and the values of κ'_{fl} and $\tan\delta$ are those given in Appendix C.

The TEM_{n00} (n = 8, 9, 10, 11) modes were used. Measured resonance frequencies for the empty tank modes are shown below.

mode	frequency
n = 8	8.209 GHz
n = 9	8.991 GHz
n = 10	10.007 GHz
n = 11	11.289 GHz

Figures 4.5 and 4.6 show the actual fill level plotted against predicted fill level V_{fl} for each of the resonant modes. For each mode, the orientation dependance can be seen as differences between the results for vertical and horizontal tank orientations. For example, mode 8 shows that vertical tank orientation causes much higher predicted fill than horizontal orientation, especially at the 50 ml fill level. This is also true of mode 9, but not for modes 10 and 11. This is due to the shifting of position of the first resonance node as frequency increases. The first node for mode 8 is located at about 0.9 cm from the tank bottom. In the vertical orientation, the fluid-vapor interface

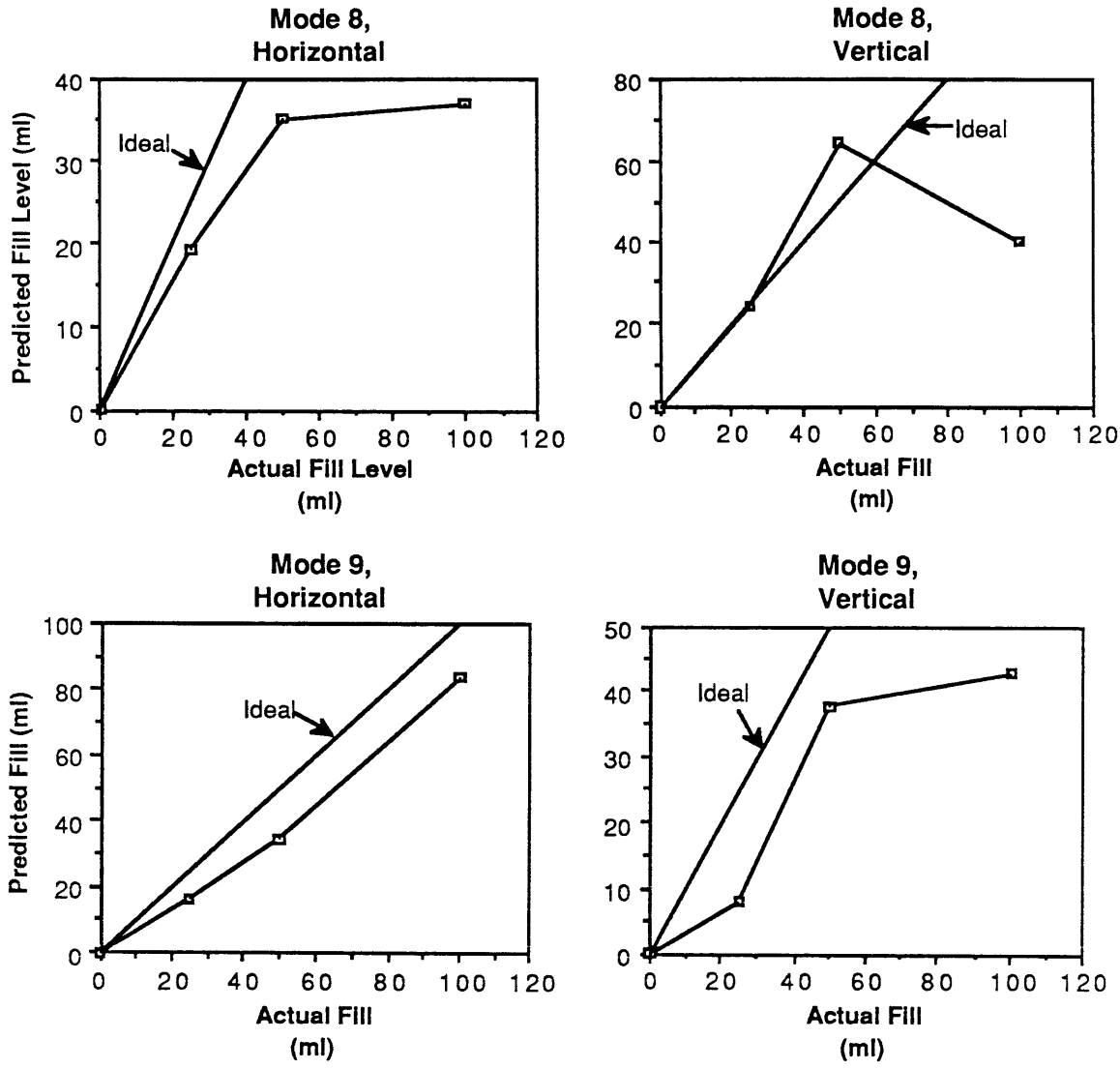

Figure 4.5 High Sensitivity Experiment Results, Modes 8 & 9

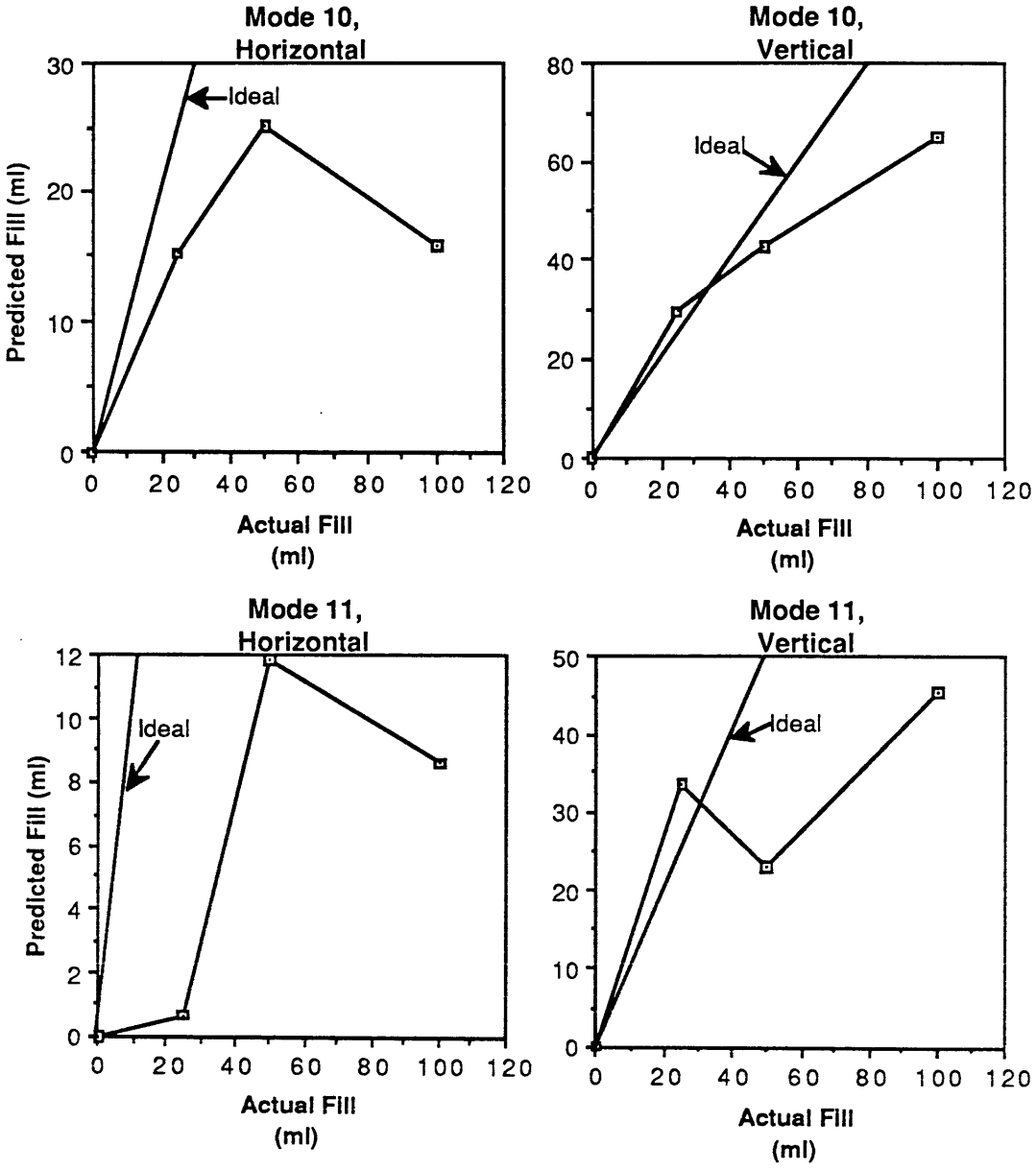

Figure 4.6 High Sensitivity Experiment Results, Modes 10 &11

passes through this node at about the 40 ml fill level. Changes in Q will appear too small as the interface passes through the node, where electric field strength (and energy dissipation) is smallest. Thus, predicted fill will appear to level off at fill levels near 40 ml. For higher frequency modes, the node occurs closer to the tank bottom, until for mode 11 it occurs at the 30 ml fill level. The position of the resonance nodes is shown with vertical predicted fill plots for the first three modes in figure 4.7.

For each tank orientation, the numerical average of the values of V_{fl} for all four modes was taken. Figure 4.8 shows the individual mode values plotted as points, while the averaged values are connected with lines. The plot shows that vertical and horizontal predicted fill are closer when averaged over four frequencies than at any one frequency. It is thought that the radial electric field variations discussed in section 4.1.1 could account for the increasing error at higher fill levels. These variations are not corrected by averaging.

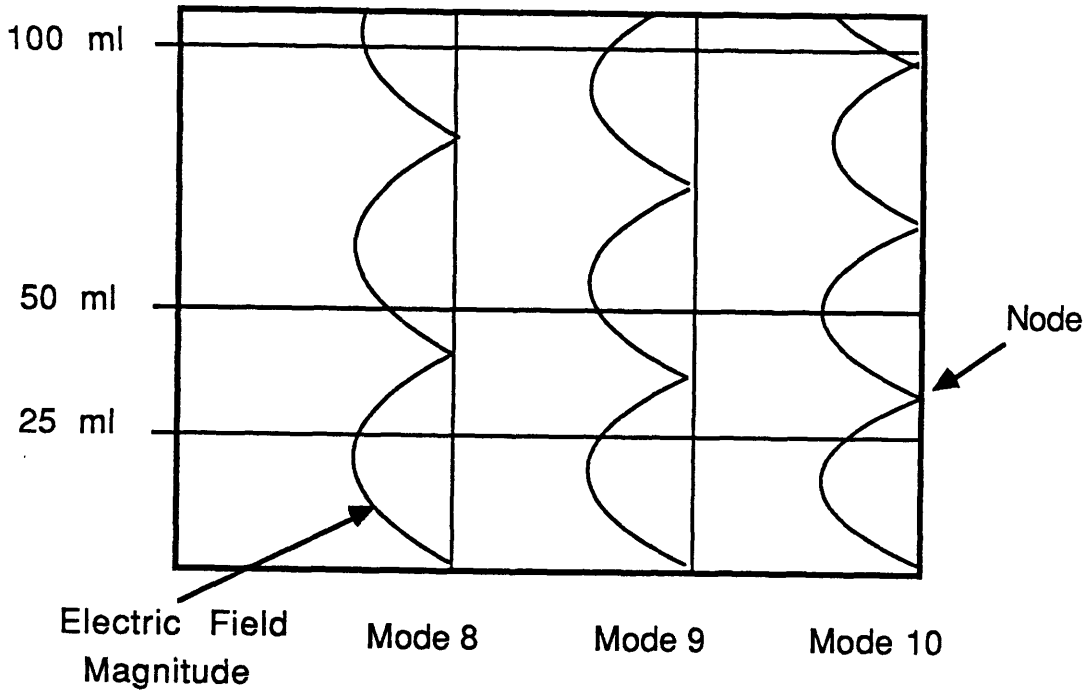

Figure 4.7 Fluid Level and Resonance Node Positions High Sensitivity Measurements, First Three Modes

Figure 4.8 Ethyl Mode Averaged Fill Level

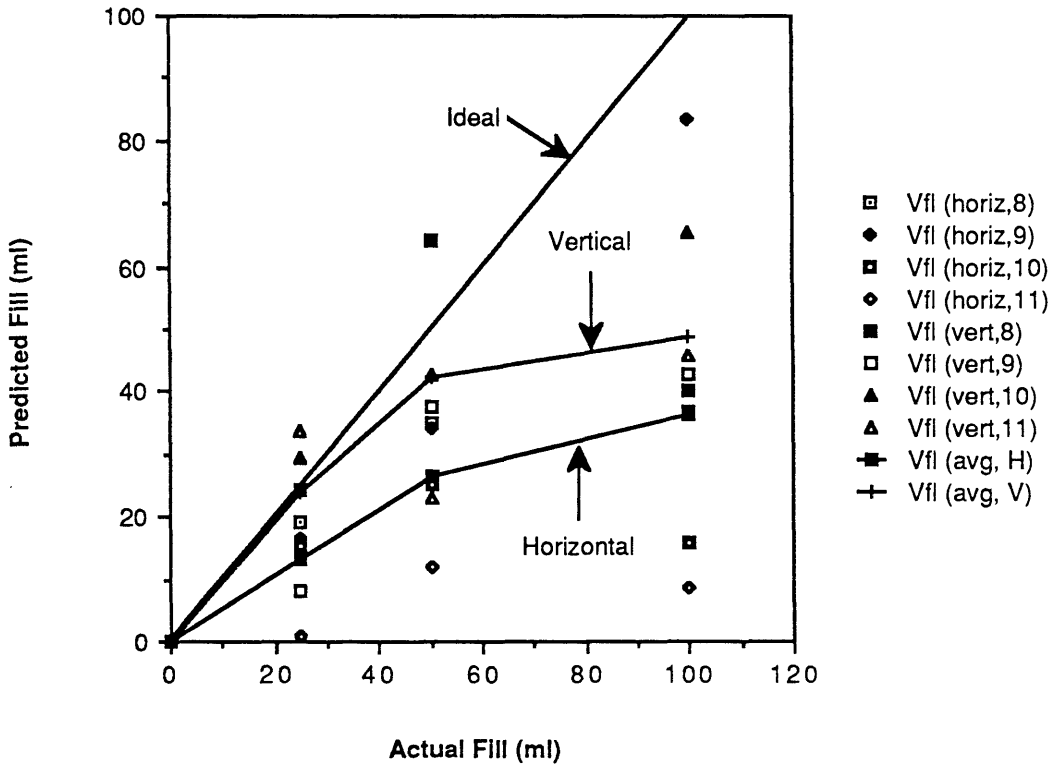

4.2 Non-Resonance Absorption Experiment

In order to simulate a large number of low gravity fluid configurations, uniformly shaped slabs of vinyl nitrile (modified PVC) closed cell foam were used instead of liquid for all non-resonance tests. This foam was used because it has a very low dielectric constant (1.31), and thus simulates liquid oxygen and liquid hydrogen well in terms of energy storage and distortion of the electric field at its surfaces, as discussed in section 2.2. The loss tangent of 0.028 is substantially higher than in these cryogens, and allowed measurement of Q changes with very simple equipment. The dielectric constant and loss tangent of the material were determined by measurement of empty and full tank Q and capacitance C. The procedure is given in Appendix C. The impedance bridge was capable of determining both Q and C with no change in the set-up.

The use of foam also allowed easy configuring of the material into various shapes. This permitted direct determination of response changes due to orientation of the tank contents.

A large variety of foam configurations were tested with the simulated fluid oriented horizontally and vertically with respect to the tank. The foam sizes used are shown in figure 4.9. Actual full tank fill level was known to ± 1.1 %, with possible error due to uneven cutting of the foam edges. The foam configurations are summarized in figures 4.10 through 4.14.

Predicted foam volume V_{fl} was calculated using the measured values of Q and the expression for fractional fill F derived in section 2.1,

$$F \equiv \frac{V_{fl}}{V_t} = \frac{\kappa'_{fl}\,(1/Q \;-\; 1/Q_{mt})}{\tan\delta \;+\; (\kappa'_{fl} \;-\; 1)/Q}$$

where $V_t = 58.52$ liters

$\kappa'_{fl} = 1.31$

$\tan\delta = 0.028$

The values of dielectric constant and loss tangent were not known with great certainty, due to the accuracy limitations of the impedance bridge used in the measurements. Therefore, the values for predicted foam volume were normalized to

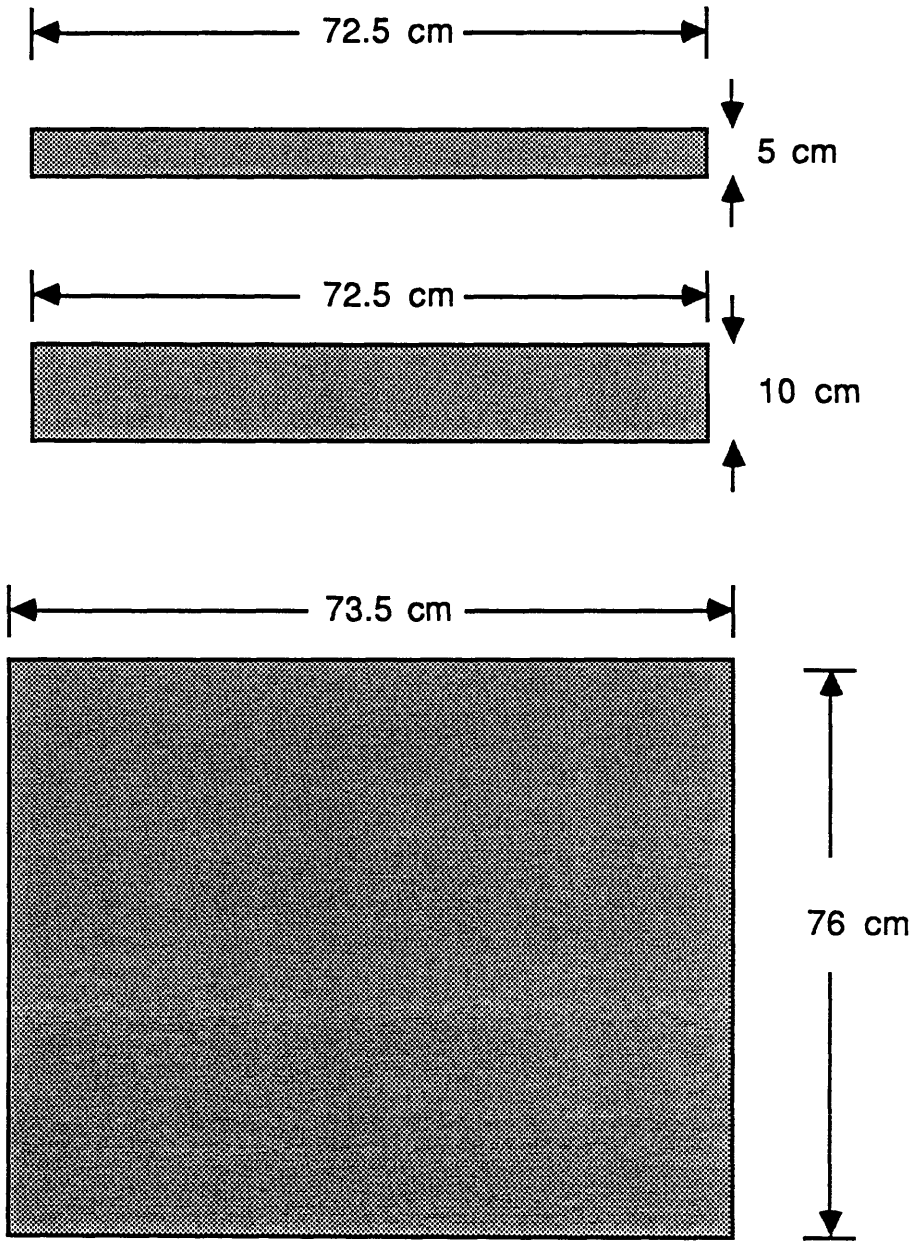

Figure 4.9 Foam Slab Sizes

(All slabs 1.9 cm thick)

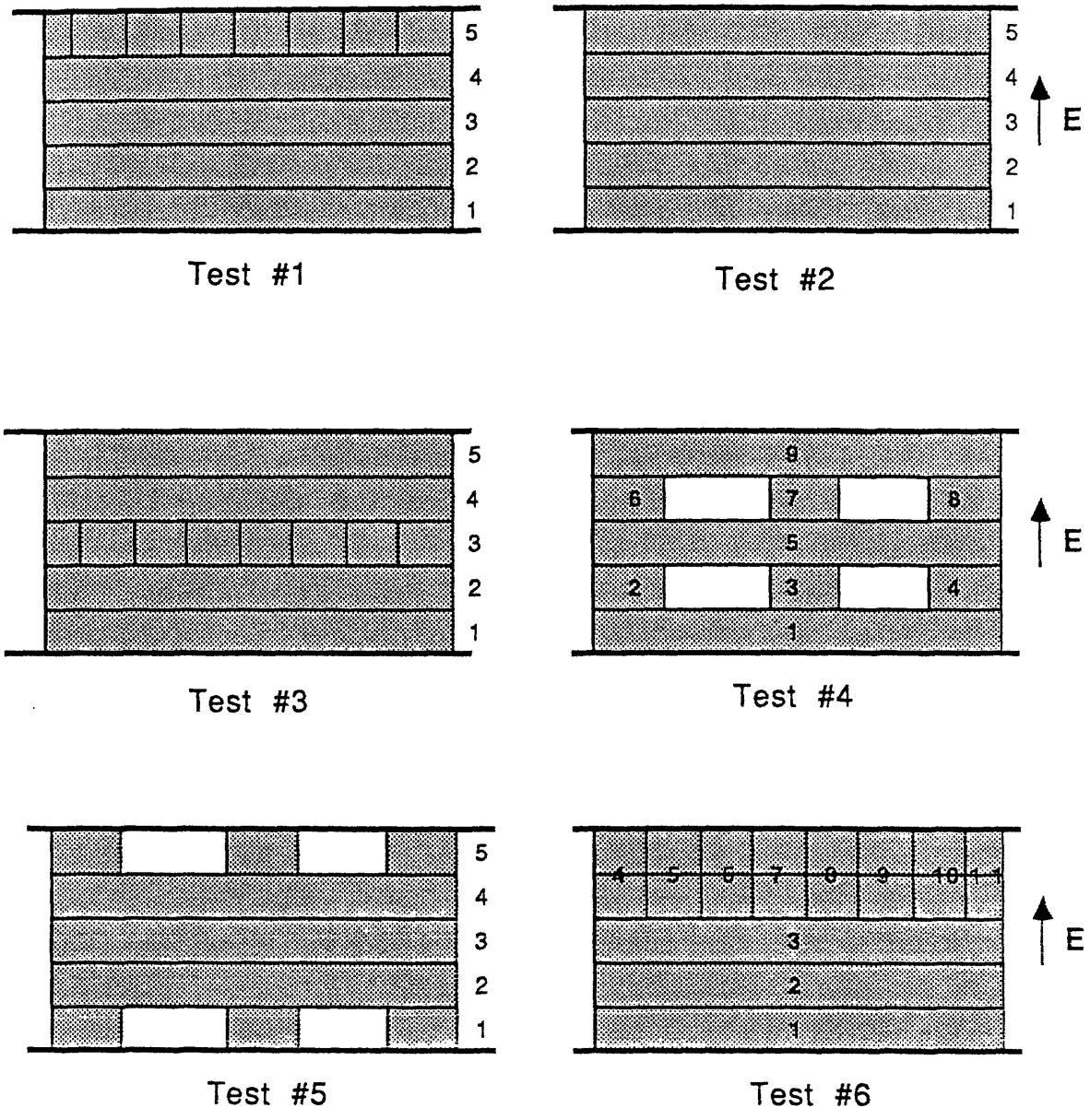

Figure 4.10 Foam Configurations
Perpendicular Tests

(front view)

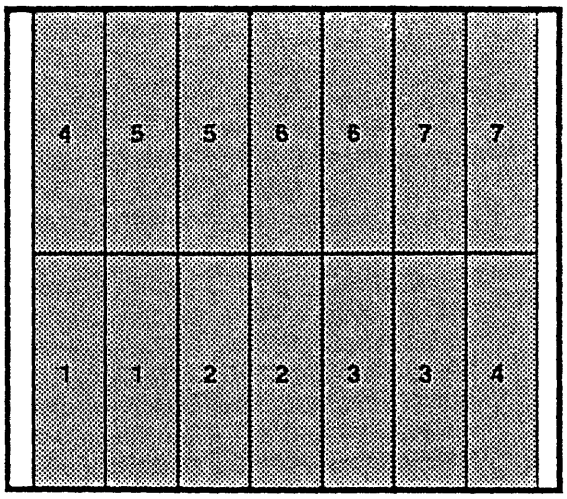

Test #7
Top View

⊕ E

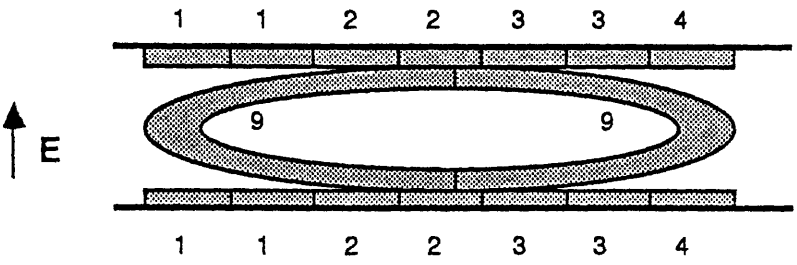

Test #7
Section
(front view)

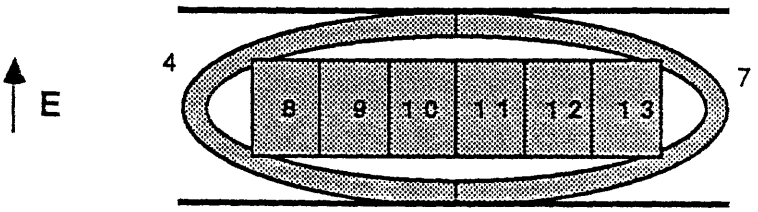

Test #7
Side View

Figure 4.11 Foam Configurations

Perpendicular Tests (cont'd)

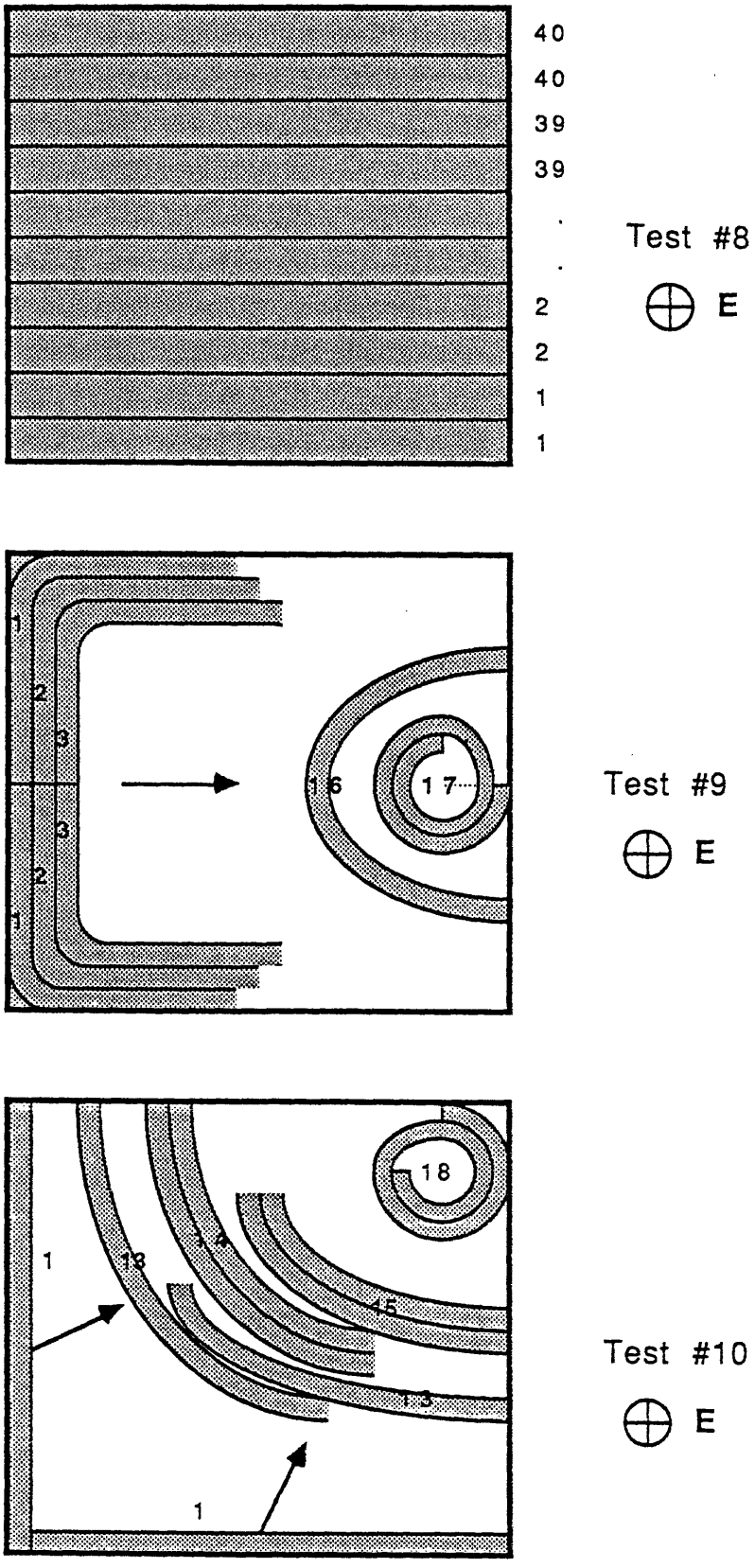

Figure 4.12 Foam Configurations
Parallel Tests (Top View)

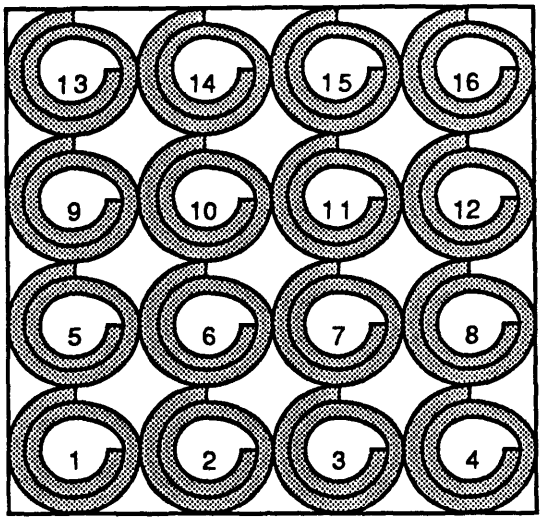

Test #11

⊕ E

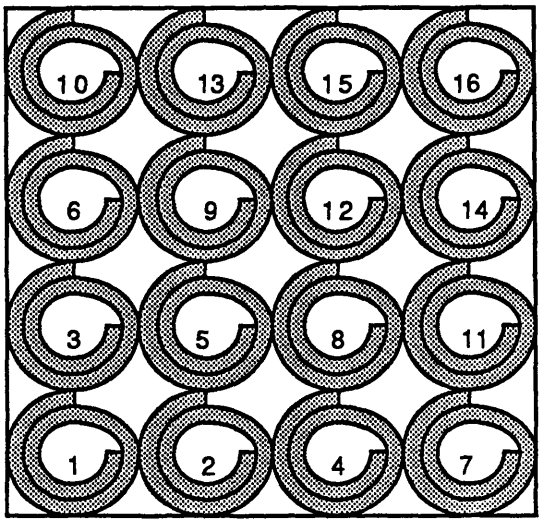

Test #12

⊕ E

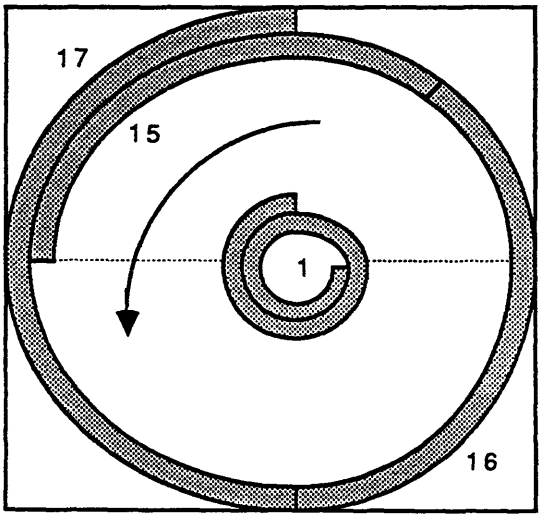

Test #13

⊕ E

(top view)

Figure 4.13 Foam Configurations

Parallel Tests (cont'd)

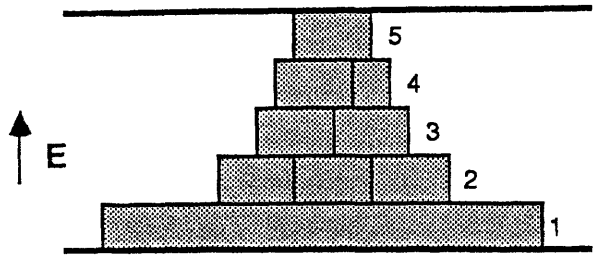

Test #14

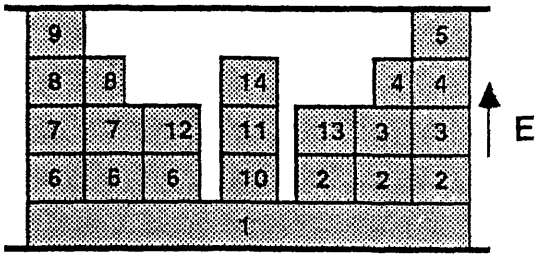

Test #15

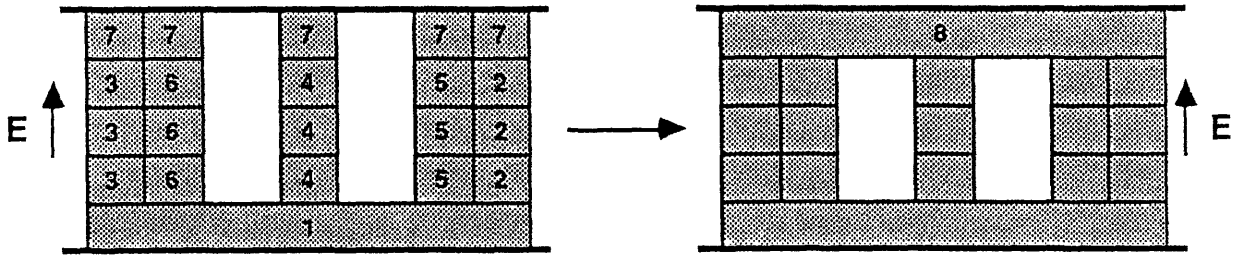

Test #16

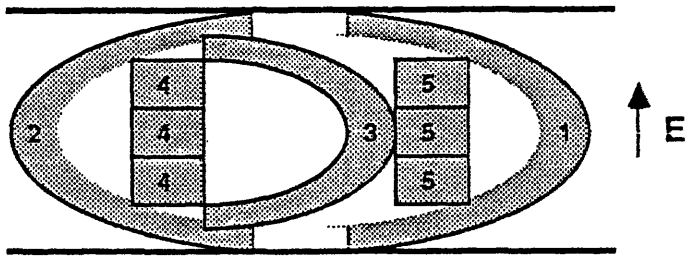

Test #17

Figure 4.14 Foam Configurations

Parallel Tests (cont'd)

(front view)

full tank values.

A calibration run was performed in order to establish the effect on the measurements of different tank orientations within the laboratory. Tests were performed using identical foam configurations with the tank in different positions with respect to the laboratory. The difference in predicted foam volume was less than 1% for all fill levels. When normalized to full tank, the difference in predicted foam volume was less than 0.2% for all fill levels.

The tests are devided into two general categories. The first includes those foam configurations for which most of the surface area exposed during filling is oriented perpendicular to the applied electric field lines, as shown in figure 4.15a. Tests 1-7 fall into this category. The second category includes those tests for which most of the exposed surface area is oriented parallel to the applied electric field, as shown in figures 4.15 b and c, and includes tests 8-17. Tests in the first category will be called 'perpendicular tests', while the remainder will be called 'parallel tests'.

This classification is made based on observation of the plots shown in figures 4.16 through 4.32. The perpendicular tests (tests 1-7) show substantial position independance for all foam configurations. These are shown in figures 4.16 through 4.22. All observed errors are well within the accuracy of the measurement instrument. Test 2 (figure 4.17) demonstrates this, as the foam configuration was the same as in test 1 (figure 4.16). A maximum error of 6% occurs at the 21 liter (36%) fill level. This is attributed to the limit of repeatability in the measurement of Q. Similar errors can be seen in tests 4 and 6 (figures 4.19 and 4.21). The mean error for normalized predicted fill volume in the perpendicular tests was $\pm$ 1.75%, despite the much lower accuracy of the bridge in determining Q, dielectric constant, and loss tangent, and the uncertainty of 1.1% in actual full tank volume. Mean error in non-normalized predicted fill volume for the perpendicular tests was $\pm$ 2.5%, demonstrating the reduction of error due to uncertainty in dielectric constant and loss tangent achieved by normalization.

The parallel tests (tests 8-17) are shown in figures 4.23 through 4.32. Mean error for normalized predicted fill volume in these tests was 8.2%. All these tests have the same general behavior, despite different foam configurations. In each, predicted fill is high, and appears to reach a maximim when the highest percentage of exposed surface area is parallel to the electric field. This indicates that fringe effects at the foam edges are contributing to non-uniformity in the electric field, despite the small dielectric constant. Boundary conditions at the foam surfaces permit the electric field lines to remain uniform when the surface is perpendicular to the applied field (tangential E is zero). However, when the foam surfaces are parallel to the applied field, boundary

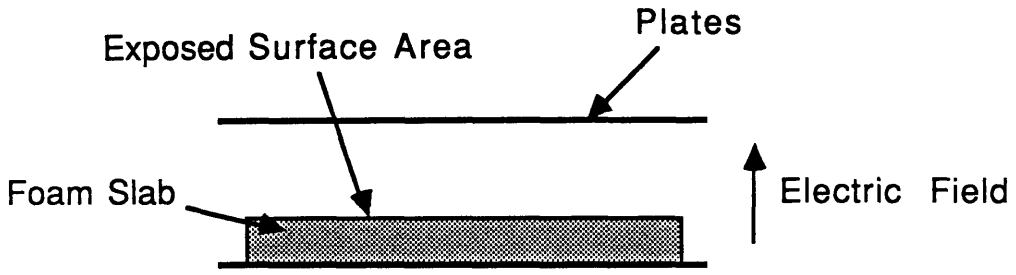

a. Front View, Perpendicular Field

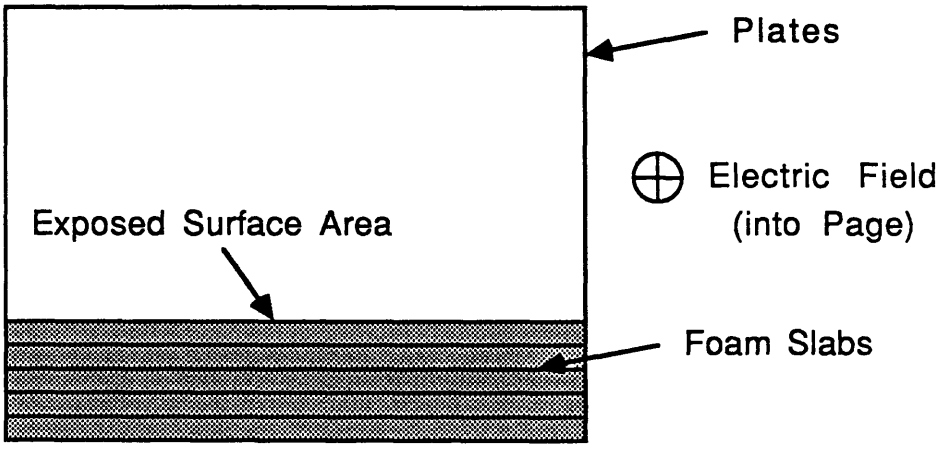

b. Top View, Parallel Field

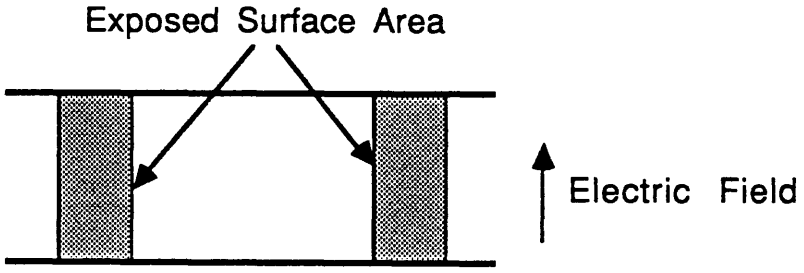

c. Front View, Parallel Field

Figure 4.15 Perpendicular and Parallel Test Definitions

Figure 4.16 Foam Test #1

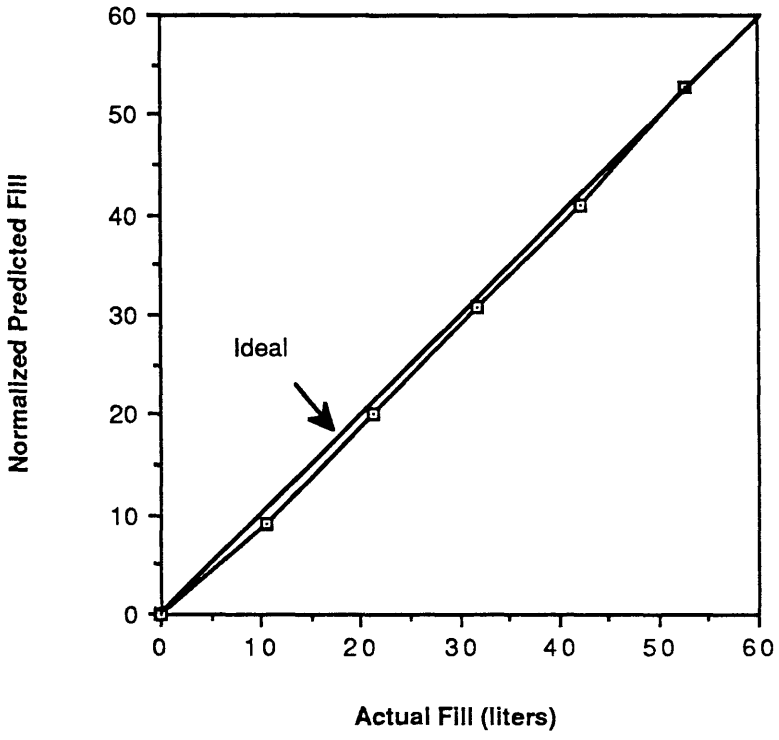

Figure 4.17 Foam Test #2

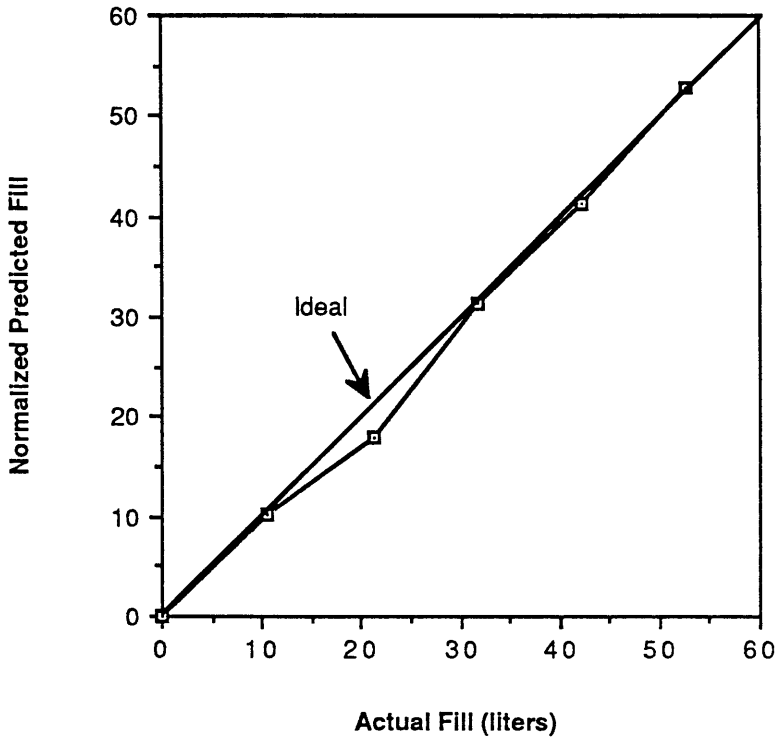

Figure 4.18 Foam Test #3

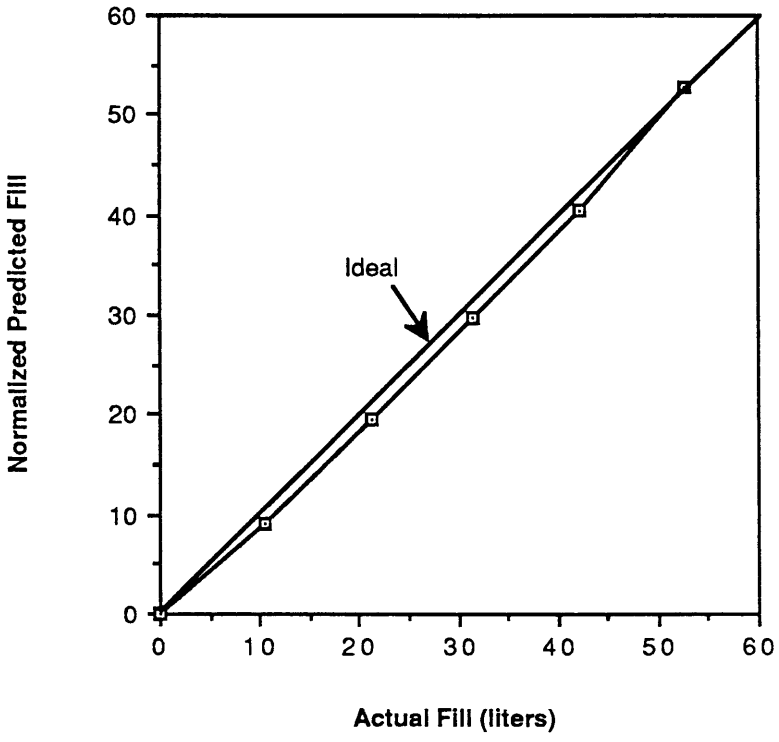

Figure 4.19 Foam Test #4

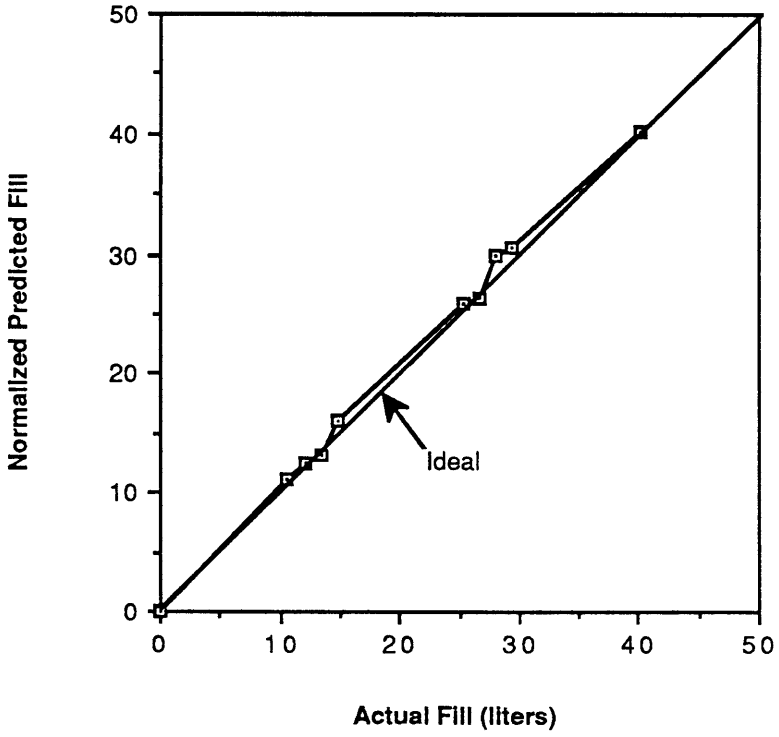

Figure 4.20 Foam Test #5

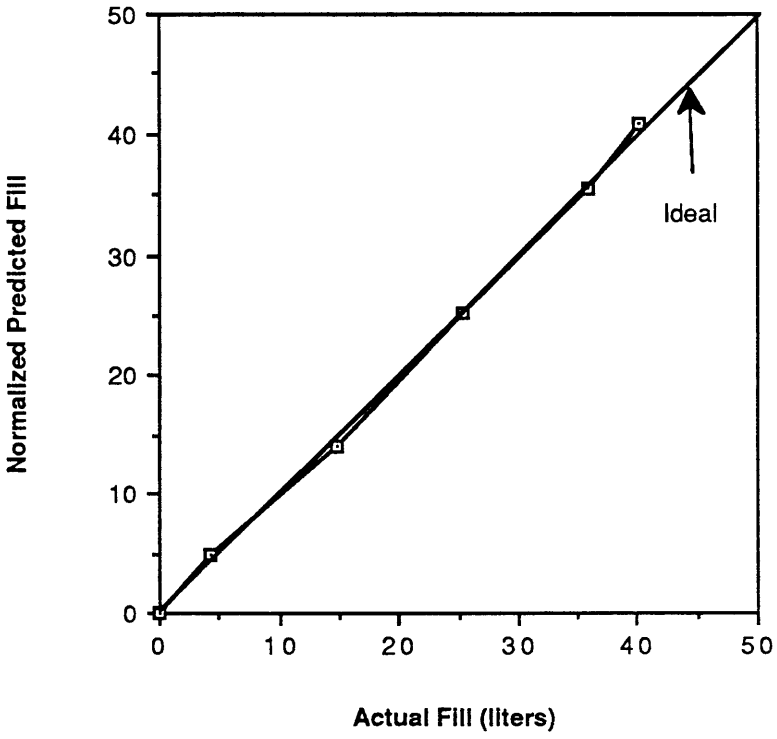

Figure 4.21 Foam Test #6

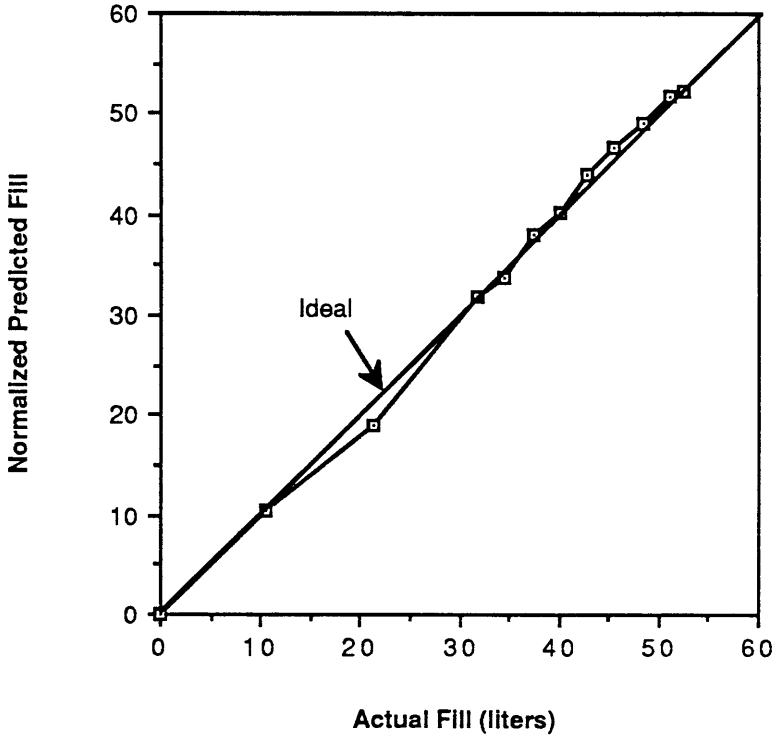

Figure 4.22 Foam Test #7

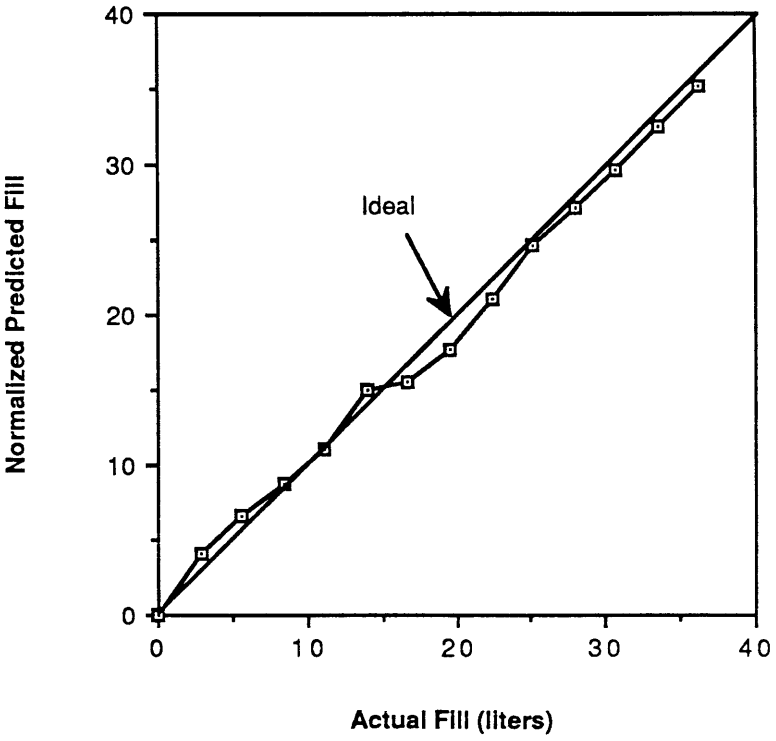

conditions require that the field lines at the surface are continuous. The field is thus distorted as discussed in section 2.2.1. This results generally in decreased energy storage in the air. Predicted fill is therefore higher than the ideal, which assumes uniform fields.

Test 8 (figure 4.23) shows the fringing effect. As the foam surface passes roughly the 28 liter fill level, the error is at a maximum. Tests 9 and 10 (figures 4.24 and 4.25) have similar behavior. These configurations were designed to simulate typical low Bond number meniscii. Tests 11 and 12 have substantially more exposed surface area, and all this area is parallel to the field lines. This extra surface area accounts for the additional error seen in predicted fill for these tests, when fringing effects are considered.

Test 13 shows that interaction with the fringe effects due solely to the plate edges is minimal. In this test, fill began in the center of the tank, and continued outward. Errors induced by plate fringing would have been increasingly visible as the tank was filled. Instead, the behavior is very similar to that seen in test 8, in which the tank was filled from one edge to the other.

Tests 14-17 (figures 4.29 - 4.32) show the same general behavior as the other parallel tests, despite the difference in the way the tank was filled in each case. When compared with the other parallel tests, these show that position dependance in the low frequency method is good, limited mainly by the fringing effects discussed above.

Tests 16 and 17 (figures 4.31 and 4.32) show error increasing almost linearly with fill. Test 16 began with a large slab, which was followed by smaller slabs in groups of three, stacked one on top of the other. With each added group of smaller slabs, the error in predicted fill can be seen to increase. The eighth layer was actually a single large slab which replaced the smaller slabs in layer seven. Although only a small volume of foam was added, error was reduced. This can be attributed to the removal of the five small pieces and their edge effects. Test 17 shows curved slabs for the first three layers, with approximately 5% error at 35 liter (60%) fill. This can be compared to the first three layers of test 1, which used the same sized slabs oriented flat and against the plates. At 60% full, test 1 had 1.8% error. The increase is thus attributed to the surface curvature, and the related fringing effects.

Figure 4.23 Foam Test #8

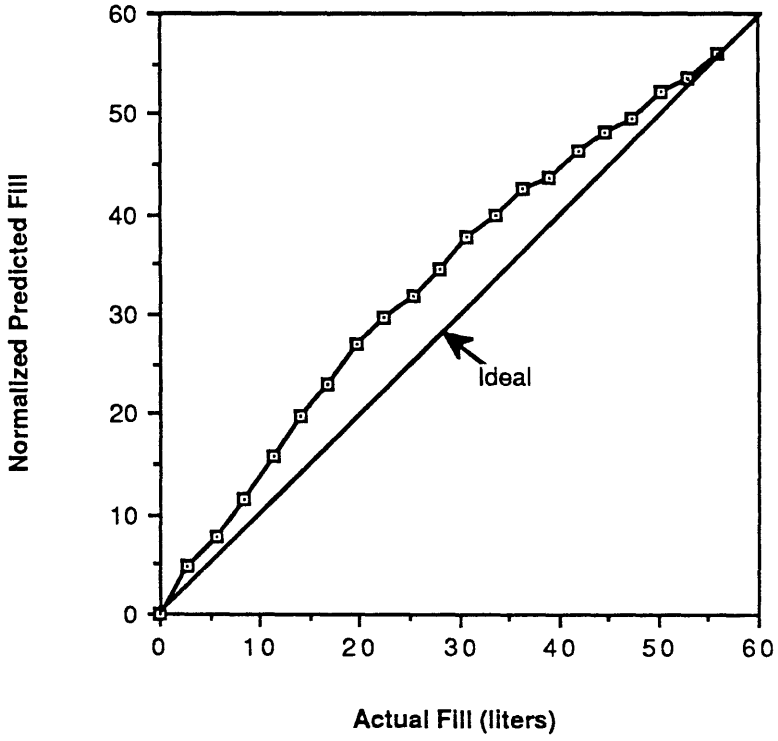

Figure 4.24 Foam Test #9

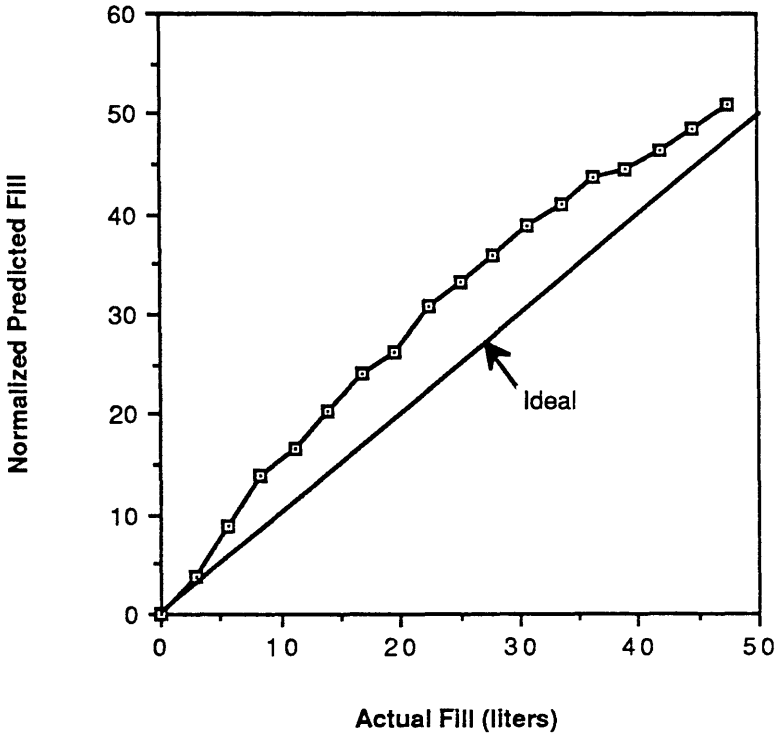

Figure 4.25 Foam Test #10

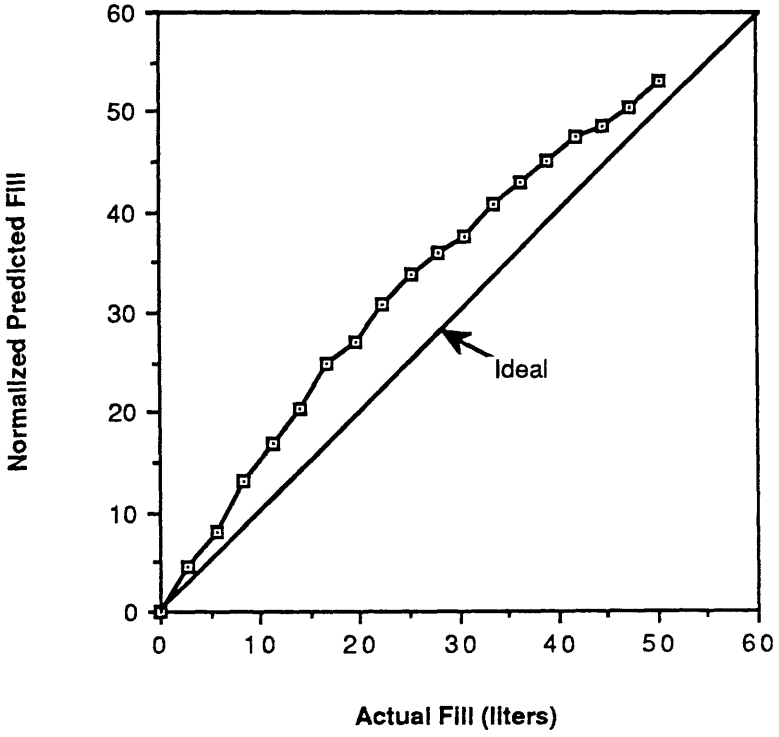

Figure 4.26 Foam Test #11

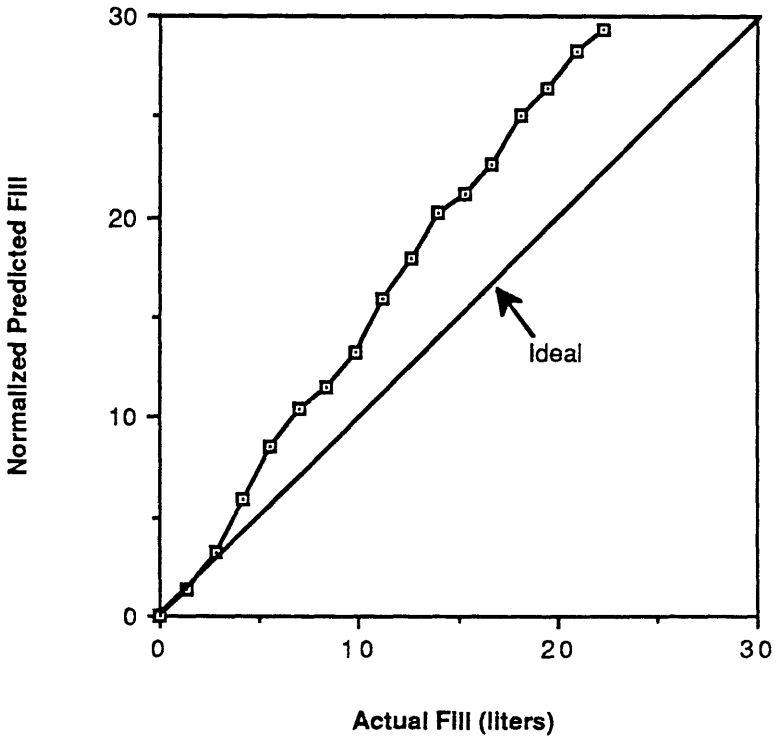

Figure 4.27 Foam Test #12

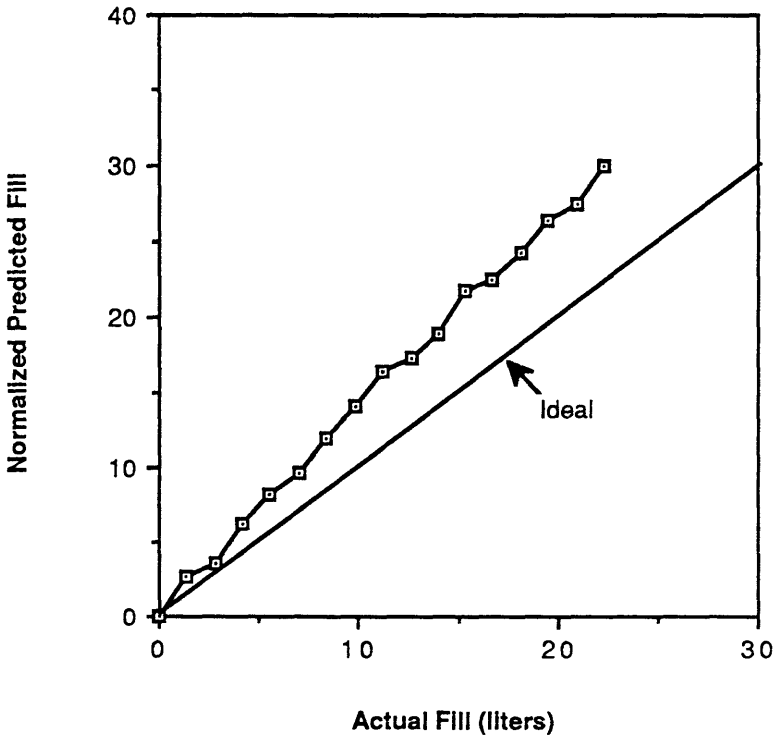

Figure 4.28 Foam Test #13

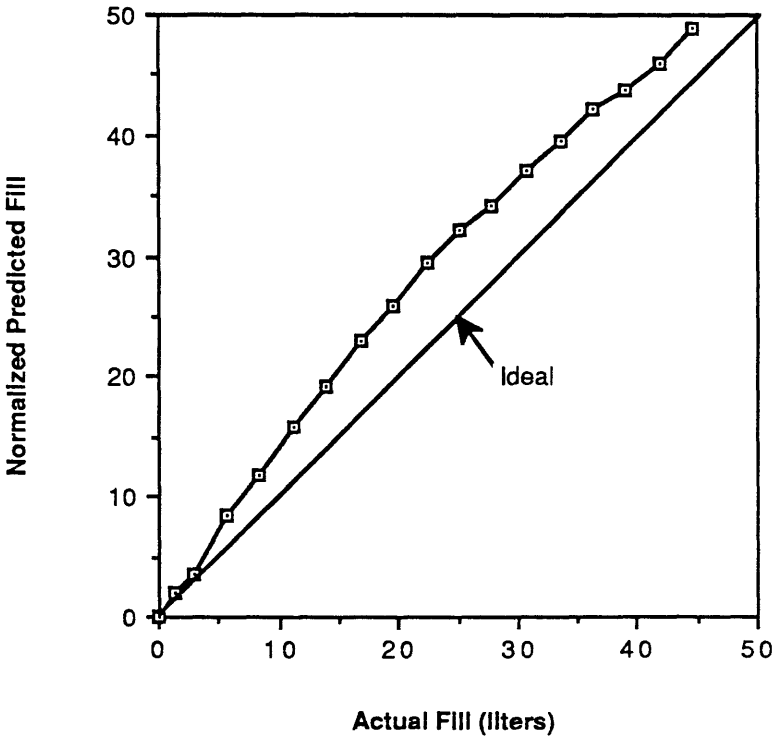

Figure 4.29 Foam Test #14

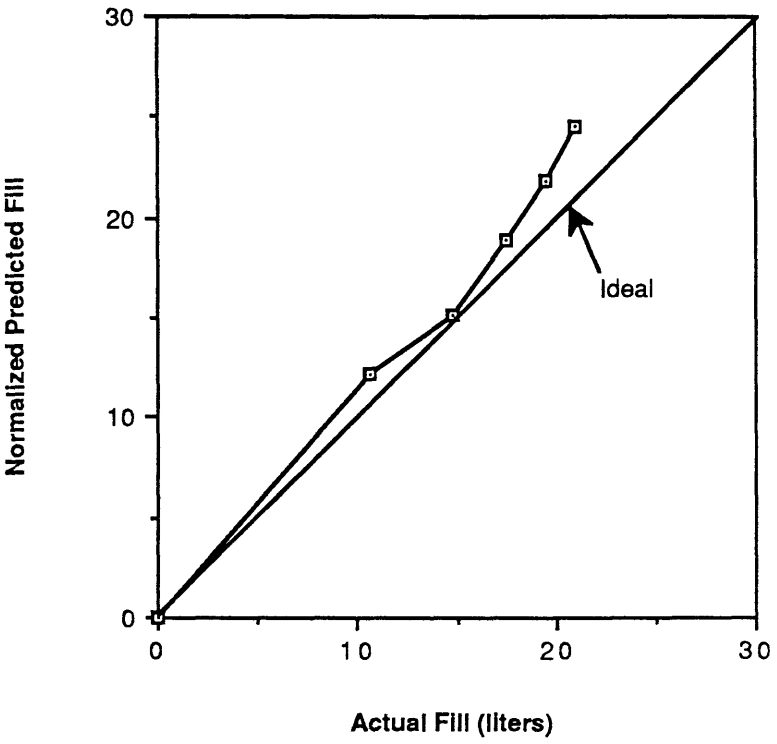

Figure 4.30 Foam Test #15

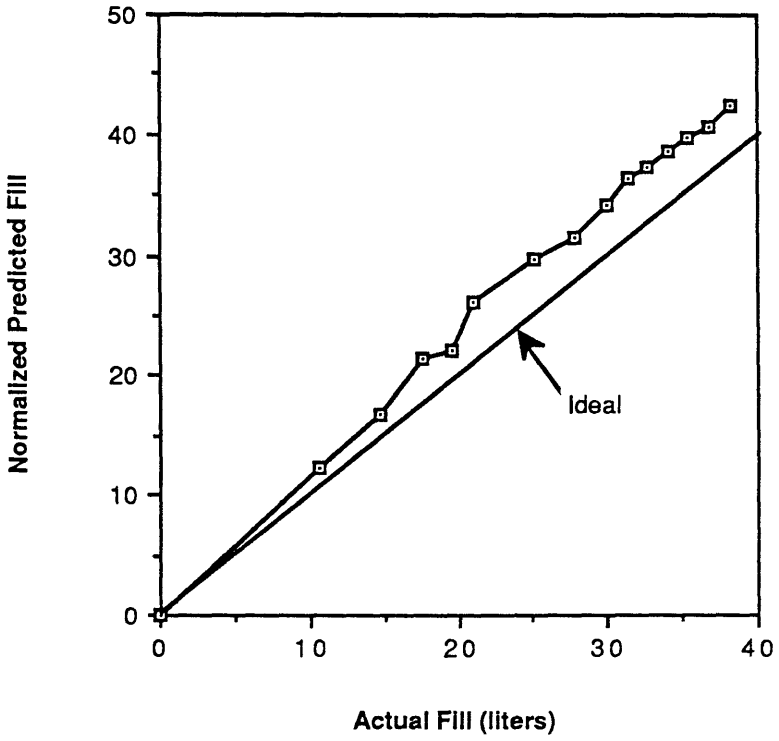

Figure 4.31 Foam Test #16

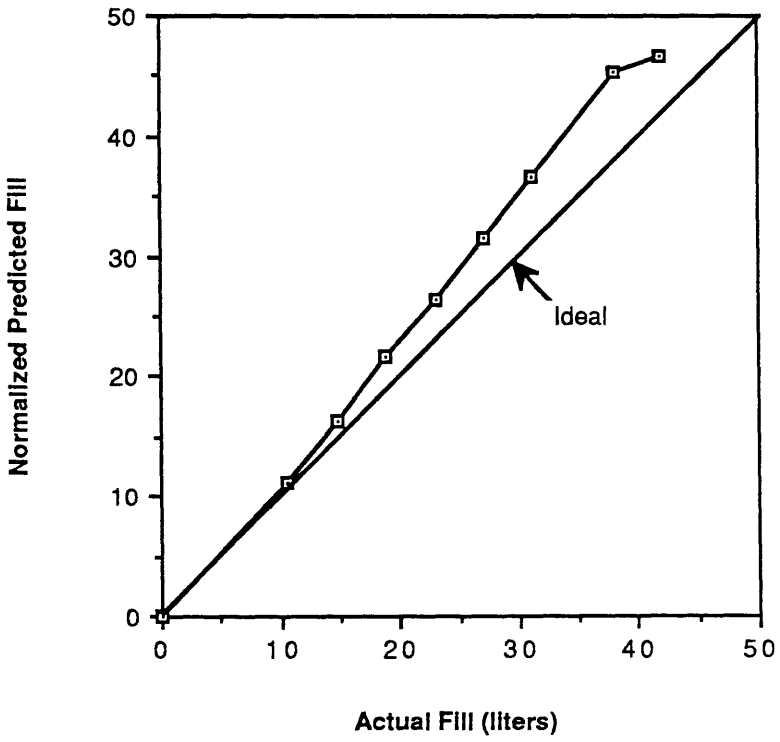

Figure 4.32 Foam Test #17

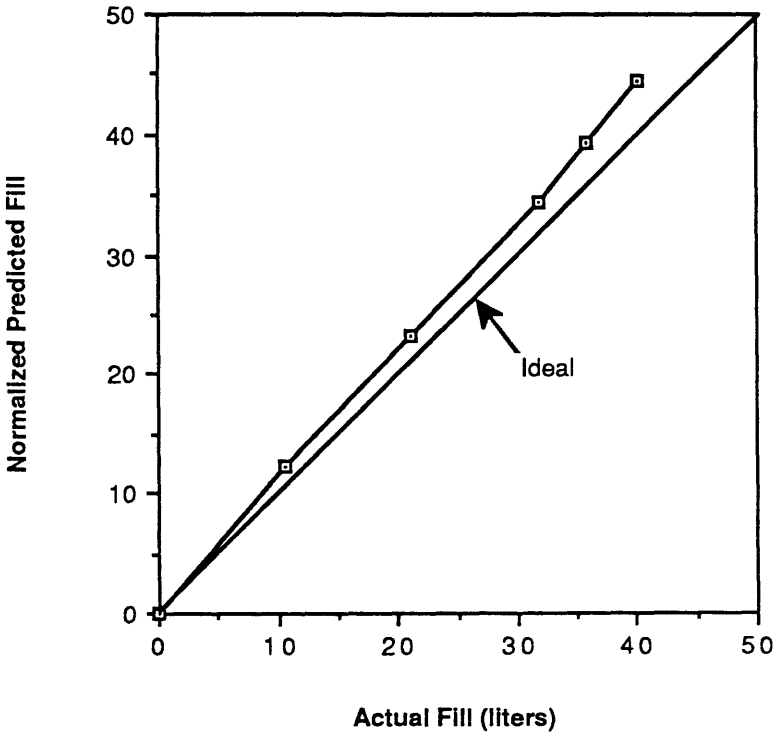

Chapter 5

Conclusions

5.1 RF Resonance Absorption Experiment

In this experiment, loss measurements made at a number of resonant frequencies were used to predict fluid volume in a coaxial right circular cylinder. The measurements were performed with both low and high loss tangent liquids.

For both liquids, fill volume predicted from loss measurements made at a single resonant frequency depended on fluid orientation. Differences were thought to be due to spatial non-uniformity of the resonant electric field structure in the tank.

A reduction of the orientation dependance was observed when predicted fill was averaged over a number of frequencies. Error remaining in averaged fill level was thought to be due to the radial variation of electric field within the tank. This error was not reduced by averaging.

5.2 Non-Resonance Absorption Experiment

In this experiment, loss measurements were taken well below resonance in a tank configured as a parallel plate capacitor. Foam was used instead of liquid, in order to simulate liquid oxygen and liquid hydrogen in a large variety of orientations within the tank.

For a large number of foam configurations, substantial orientation independance was observed. When the majority of exposed surface area of the foam was oriented perpendicular to the applied electric field, predicted foam volume had a mean error of $\pm$ 1.75%, despite much larger inaccuracy ($\pm$ 7.5%) in the measuring instrument. When the majority of exposed surface area was oriented parallel to the applied field, mean error in predicted fill was $\pm$ 8.2%. This error was attributed to fringing effects at the edges of the foam slabs.

Appendix A

Electrical Properties of Liquid Oxygen and Liquid Hydrogen

This thesis is devoted primarily to electromagnetic methods of fluid quantity measurement, and so the elctrical properties of liquid oxygen and liquid hydrogen are of critical importance. Electrical energy storage and dissipation in the fluid (and in the tank-fluid system) depend on these properties, which themselves vary with the purely physical properties of temperature, pressure, density, etc. Therefore, accurate fluid quantity gauging requires understanding of the electrical properties of these fluids.

The relevant fundamental electrical property for electromagnetic fluid gauging methods is the complex permittivity. From this quantity, the more measureable variables of quality factor, Q, and dielectric constant can be derived. These concepts are developed more fully in section 2.1, however general definitions are given below.

The complex permittivity, or dielectric constant, is composed of two parts, the real part ε' and the imaginary part ε'' and is expressed as $\varepsilon = \varepsilon' - j\varepsilon''$. The real part is a storage term, while the imaginary part is a loss term. The permittivity of vacuum is purely real (no loss), and is used as a reference. It has the value $\varepsilon_0 = 8.85 \times 10^{-12}$ Farads/meter. The ratio $\varepsilon/\varepsilon_0$ is called the relative complex permittivity, and leads to the following definitions:

$$\kappa' \equiv \frac{\varepsilon'}{\varepsilon_0} = \text{relative permittivity}$$

$$\kappa'' \equiv \frac{\varepsilon''}{\varepsilon_0} = \text{relative loss factor}$$

$$\tan\delta \equiv \frac{\kappa''}{\kappa'} = \frac{\varepsilon''}{\varepsilon'} = \text{loss tangent}$$

The real part of the relative complex permittivity is often implied when the term 'dielectric constant' is used.

If a spacecraft fuel tank is constructed as a capacitor, as shown in figure A-1,

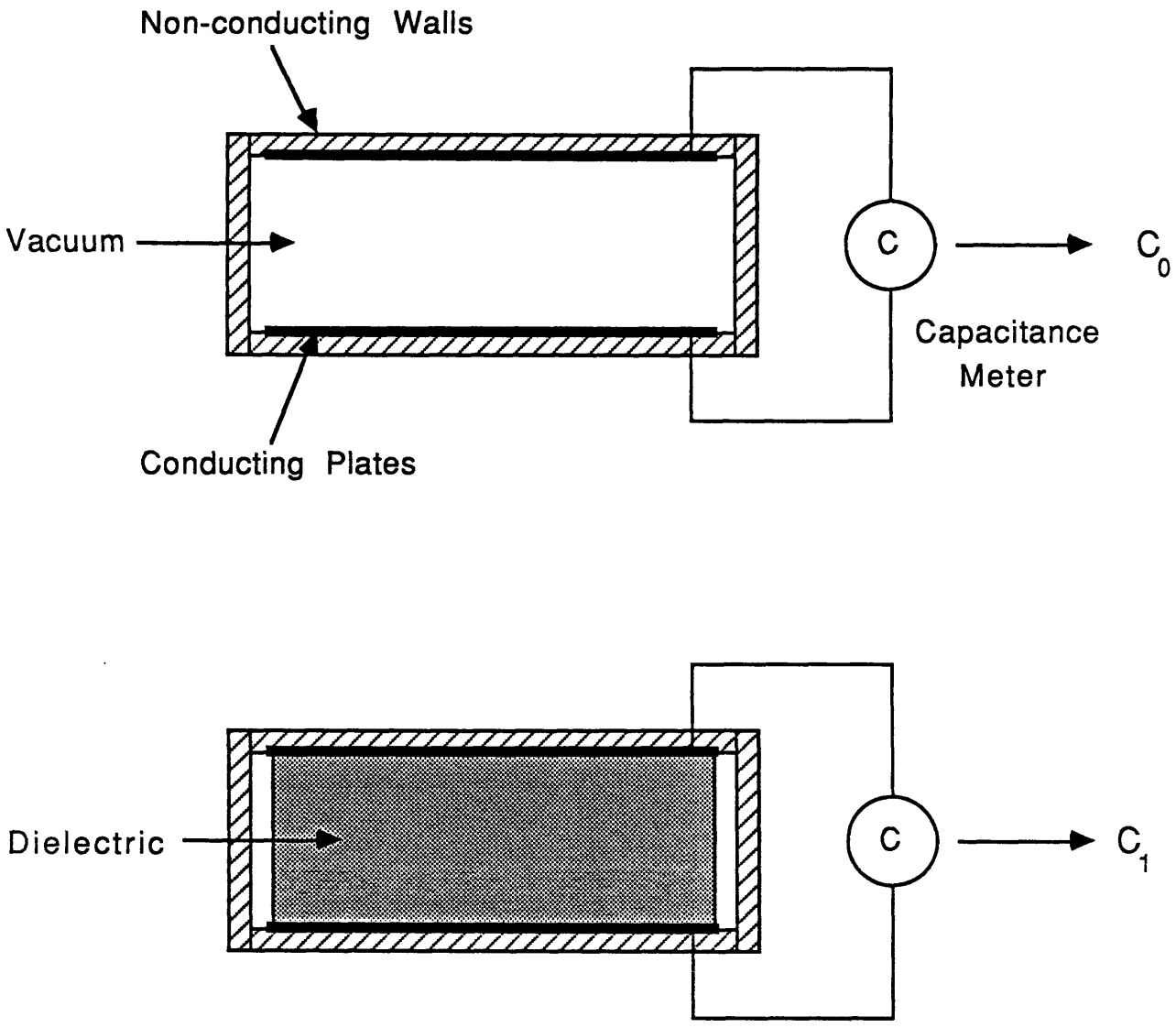

Figure A-1 Fuel Tank Constructed As Parallel Plate Capacitor

the real part of the dielectric constant can be thought of as the ratio of the capacitance C_1 of the tank filled with dielectric ε_1 to the capacitance C_0 of the same tank with vacuum replacing the dielectric, or

$$\kappa' = \frac{C_1}{C_0}$$

This relation makes κ' easy to measure, and thus this parameter has become widely used to describe dielectric materials. The impact of dielectric constant on simple capacitive gauging methods is clear from this definition, but it should be noted that energy storage and electric field strength within the tank contents will also be proportional to dielectric constant. This makes κ' important in all RF gauging techniques.

Dielectric constant in LO_2 and LH_2 has been well documented. One can find values of κ' for the most common temperatures and pressures, at frequencies between DC and the infrared region [14 - 20]. The most common values given are the static (DC) values $\kappa'_S = \varepsilon'_S/\varepsilon_0$. Values of static dielectric constant for other temperatures and pressures can be calculated from the Clausius-Mosotti relation [11], valid when the molecules are non-polar (no space charge distribution of their own) or when they are arranged in either complete disorder or in a highly symmetric array. This makes the Clausius-Mosotti model valid for LO_2 and LH_2 which are non-polar by nature. Values of the Clausius-Mosotti function and dielectric constant for liquid oxygen at various temperatures, pressures, and densities can be found in the literature [16, 18, 19]. Values of dielectric constant for LO_2 and LH_2 are given in table A for typical temperatures [21].

Table A

Fluid	Temperature	κ'(static)	Loss Tangent	Frequency
Liquid Oxygen	80°K	1.510	9×10^{-4}	3.218 GHz
Liquid Hydrogen	20°K	1.23	$< 1 \times 10^{-7}$	3.00 GHz

Also given in table A are values for loss tangent, sometimes called the dissipation factor. This quantity is widely used to describe the degree of loss of electric energy to be expected in a material. Simple models of dielectric loss predict that loss factor will be zero for non-polar liquids such as LO_2 and LH_2. This arises from the

assumption that a molecule which has no permanent dipole moment will not respond in any way to an applied electric field. It has been observed, however, that a minimum loss is present even in the purest non-polar material [22]. It is theorized that this results from thermal vibrations interacting to distort a normally symmetric electron cloud. Furthermore, it is expected that this loss will be substantially constant over a wide frequency range.

There are also loss peaks observed for liquid O_2 and H_2 in the optical and infrared regions, resulting from resonances in the molecular bonds [23]. It is believed these resonances are the result of induced dipoles created when frequencies are high enough to interact with the individual atoms or sub-atomic particles [22, 24 - 28]. The resonance frequencies result from the characteristic 'relaxation time' taken for the molecule to return to normal after the applied field is removed. Debye predicts that collision with other molecules, as in a liquid, will change the relaxation time slightly, and the observed result across a large number of molecules is a broadening of the resonances into a 'relaxation spectrum'. This broadening is pictured in figure A-2. The Debye model for a system of molecules with a single relaxation time (i.e. no collisional broadening) is

$$\kappa = \kappa'_{\infty} + \frac{\kappa'_s - \kappa'_{\infty}}{1 + j\omega\tau}$$

where κ = relative complex permittivity or complex dielectric constant
κ'_s = static dielectric constant
κ'_{∞} = optical dielectric constant (frequency high enough to exclude dispersion)
τ = relaxation time

This model permits calculation of dielectric constant and loss factor at any frequency, provided relaxation time is known.

The permanant magnetic dipole moment in the oxygen molecule results in losses in the microwave region, in addition to the resonant and non-resonant losses above [29]. The reference also gives useful values of loss tangent for compressed oxygen at pressures up to 70 atmospheres.

The composite picture of loss tangent as a function of frequency, estimated

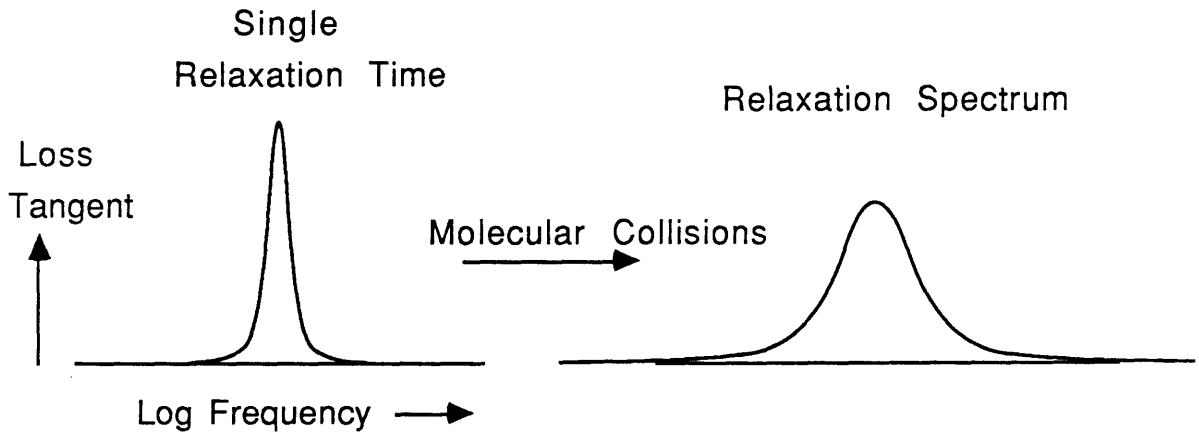

Figure A-2 Collisional Broadening

from the considerations above, is shown in figure A-3. The large losses at low frequencies are the result of the non-zero conductivity. It has been demonstrated that cryogens are essentially perfect insulators, but that charge carriers in the form of ionized molecules are constantly being created by natural cosmic radiation [30]. In the orbital environment, this source cannot be dissmissed. Also, ionic impurities present in the liquid will create an initially high value of conductivity which decreases as the ions flow out of the liquid. This is followed by the steady state current due to radiative ionization [31].

In conclusion, any fluid gauging method which relies on electrical loss in the fluid will have to have the frequency dependance of loss tangent taken into account. Extremely low frequencies should be avoided, due to the finite conductivity of fluids with ionic impurities. The advantages and disadvantages of operation in other frequency regions will have to be weighed against the ability of the system to detect small amounts of loss. Dielectric constant also has an impact on RF gauging techniques, as energy storage ocurrs in direct proportion to this quantity.

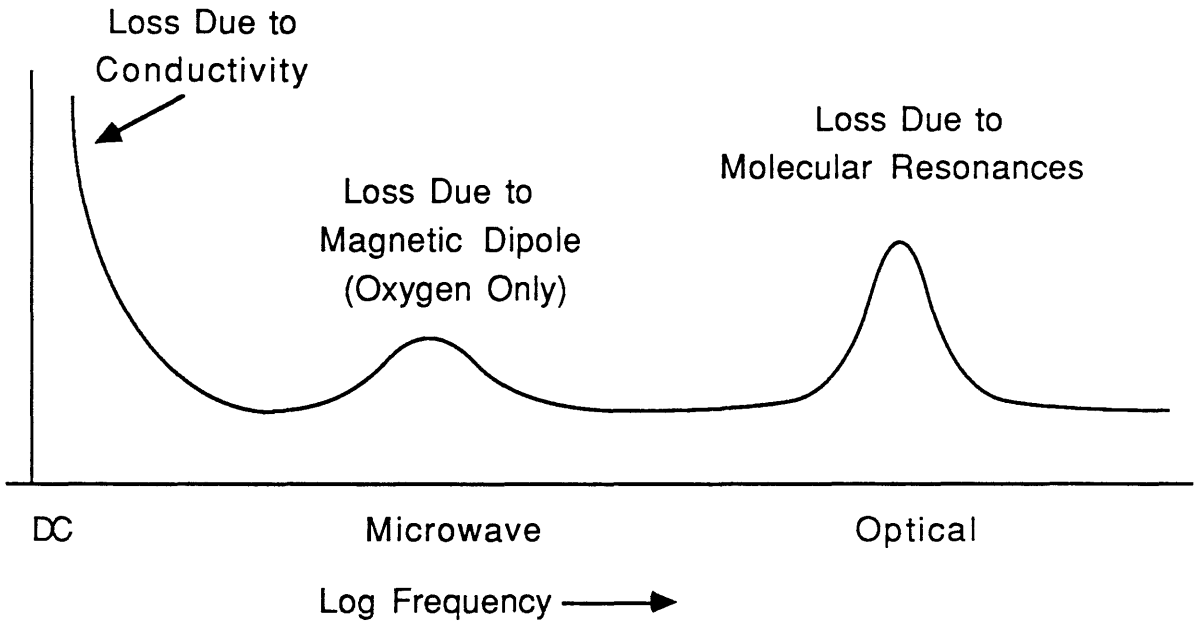

Figure A-3 Loss Tangent vs Frequency for Liquid Oxygen and Liquid Hydrogen

Appendix B

Fluid Behavior and Low-g Gauging

The primary difficulty in accurate quantity gauging in low gravity is the uncertainty in fluid location and orientation. In general, position and motion will not be known unless tank design restricts fluid behavior. Volume measurements which are influenced by fluid location will give ambiguous indications, and fluid motion will add time dependance to these ambiguities. The description of fluid behavior in low gravity is therefore separated into two regimes: hydrostatic and hydrodynamic.

Hydrostatic descriptions of fluid behavior attempt to predict how a body of liquid will behave in the steady state, i.e. with no outside forces acting on the body as a whole and after the effects of previously applied outside forces have had time to decay. For fluids in low gravity, capillary forces dominate and tend to minimize surface area. Thus the stable configurations are those with minimum surface area.

The study of hydrodynamics is concerned with the motion of the fluid body resulting from outside influences. Motion resulting from vehicle accelerations or similar 'forcing functions' is often referred to as slosh. This behavior is most often described in terms of distortion of the liquid-vapor interface relative to some standard static configuration, and is characterized by a slosh frequency and slosh mode shape.

The Bond number Bo is often used in the characterization of fluid behavior in low-g. This dimensionless quantity is the ratio of gravitational to capillary forces acting on the fluid, and is defined as

$$Bo \equiv \frac{\rho g r^2}{\sigma}$$

where ρ = fluid density
g = gravitational acceleration
r = tank radius
σ = surface tension

Figure B-1 shows how fluid orientation can depend on Bond number. For Bo>> 1, gravitational (or other acceleration) forces dominate, while for Bo << 1 capillary forces dominate. Concus [32] presents static menisci in a right circular cylinder for a complete range of Bond numbers and surface tensions.

Bo depends on r^2, and so varies considerably with tank geometry. Two different tank sizes are shown in figure B-2. The first is a 1 meter diameter cylindrical tank partially filled with fluid. In a gravity field of 10^{-3}G, Bo might be on the order of 10^{-5}G. For the same fluid in a Shuttle payload bay sized tank, Bo $\approx$ 10^{-2}G. Thus the range of Bond numbers to be expected for future space missions can be quite large.

Hydrostatic Regime

For liquid oxygen and hydrogen, and for most other fluids of interest, fluid behavior in low gravity will be dominated by capillary forces. It can be shown that the preferred liquid-vapor interface shape in this situation will be that which has the smallest capillary area [33]. This is the shape which permits the total potential energy to be at a minimum. In general this should mean that, if a number of droplets of fluid were randomly moving about the tank and colliding without too much force, they would tend to coalesce. It is therefore expected that for most tank fill levels, the majority of fluid will be contained in a single large mass, although the location and shape of this mass will in general not be known. The exception to this would be when the tank is nearly empty, and small droplets of fluid are distributed along the tank walls, held by suface tension. For most purposes this can be considered the "empty" tank state. These same energy considerations lead to both fluid droplets and vapor bubbles preferring to remain bound to the tank walls. Thus it is concluded that in the steady state the fluid mass and ullage bubble will most probably be bound to the tank wall or other internal tank structure.

Although cryogenic storage tanks will be well insulated, the possibility exists that there will be temperature gradients across the fluid body. This will give rise to a convection flow, which will tend to help the coalescing process described above by providing greater opportunity for smaller vapor bubbles to collide. Fluid droplets which are already large and wall bound will be influenced to a much lesser extent by this action. The 'steady state' will exist when this coalescing process is complete and

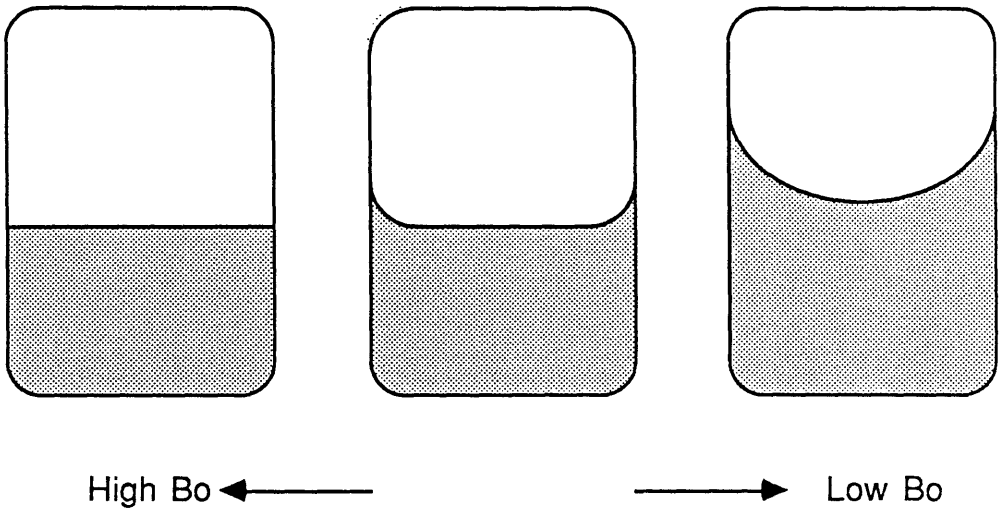

Figure B-1 Bond Number and Meniscus Shape

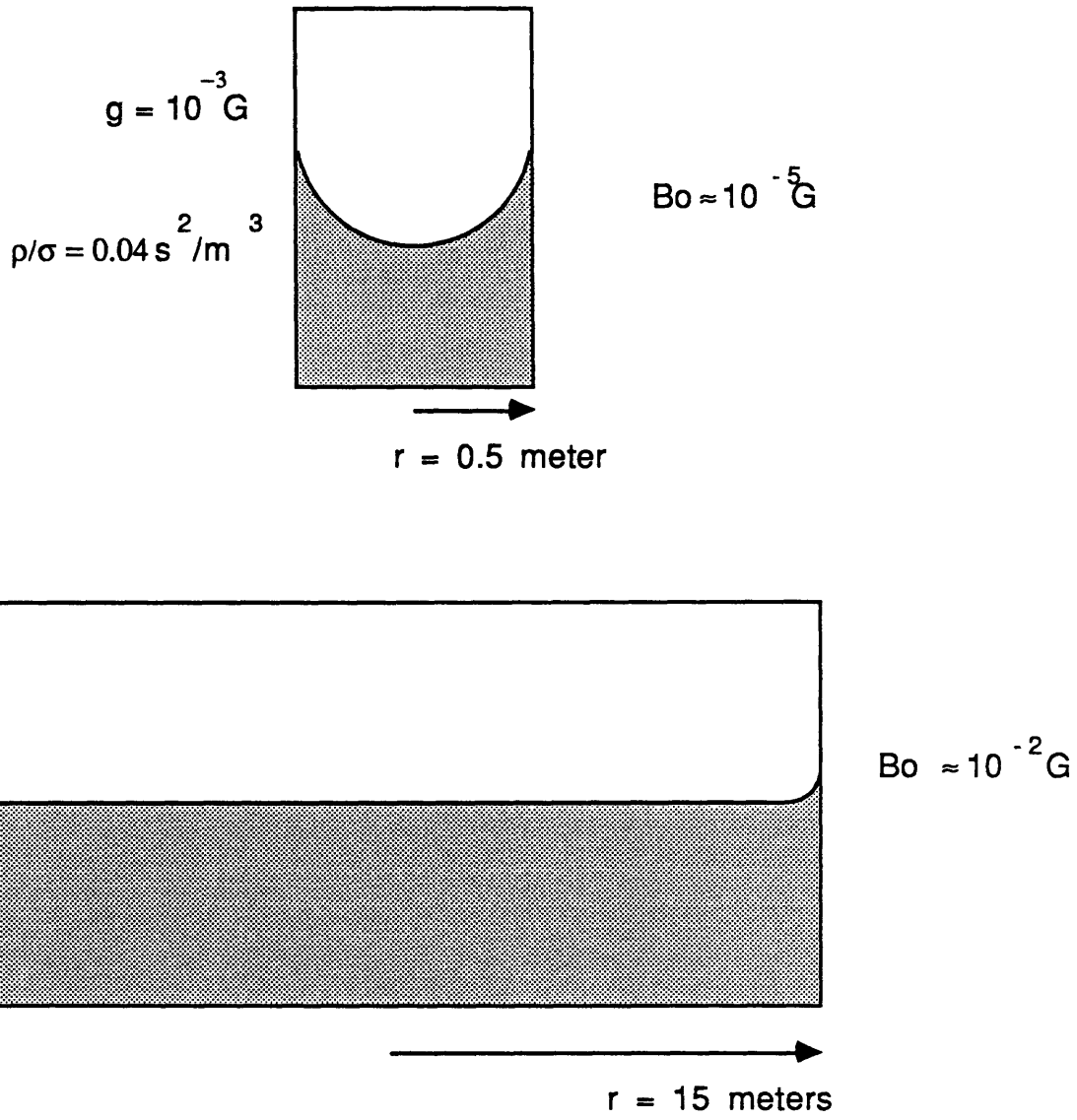

Figure B-2 Bond Number in Varying Tank Sizes

ullage and fluid are each homogeneous.

In larger tanks the effects of gravity gradients, centrifugal accelerations, and atmospheric drag can not necessarily be neglected. These are of course situation dependant, but even a small uniform acceleration such as gravity gradient could influence fluid location. References [34] provide further information on this subject. Studies in propellant reorientation are also given in the references [35, 36].

The final consideration in the hydrostatic regime is that of the liquid-vapor interface shape. Once the steady state configuration is reached, interface shape is generally determined by the requirements for minimum capillary area. It might be assumed that, for a tank symmetric about one axis, that the meniscus will also be symmetric about this axis. This will be true only if the axis of symmetry is along the larger of the tank dimensions, allowing the minimum surface area state. Unless the tank has been designed to favor a particular interface configuration despite external and internal body forces, the exact shape of the interface will not be known.

Hydrodynamic Regime

Studies of the slosh behavior of many liquids in low-g have been done, and a good body of theoretical literature exists as well [33, 37, 38]. Reference [38] provides a comprehensive summary of the literature covering low gravity fluid behavior and the associated technology, with emphasis on analytical methods of predicting liquid-vapor interface shapes and stability. Concus [39] presents a software package which calculates axisymmetric liquid-vapor interface configurations as a function of tank shape and accelerational environment. Studies have also been done which examine fluid behavior during draining and filling in low-g [39-43].

It is found that the liquid vapor interface configuration will not be known to any degree of certainty at any specific time during sloshing, and that in fact the shape might be highly nonlinear. Large amplitude breaking waves have been observed occurring in laterally excited circular cylindrical tanks [44]. These effects appear when the excitation is large, and when the excitation frequency approaches the resonant frequency of the interface itself. Similar non-linearities are observed in spherical, long rectangular, and compartmentalized circular cylindrical tanks [45-48]. They can occur in tanks of any geometry if the excitation amplitude is large enough, or if baffling devices heavily damp fluid motion

It is known that vortex formation can occur during roll maneuvering or other inertial changes, resulting from viscous action of the fluid on the tank walls. Also, draining the tank can induce vortices as well [49]. This behavior requires the use of baffles and complicated aquisition devices to control vortex formation and regulate flow during draining. These devices impact the fluid orientation picture by constraining fluid location somewhat without restricting slosh mode shape to any easily predictable configuration. One of the most successful aquisition systems is the "total communication system". This is used in applications where a continuous fluid feed is required with no accelerations applied to the body as a whole (i.e. a non-propulsive system). A large screen system is in contact with the bulk of the liquid at all times. Typically these are formed into channels positioned circumferentially inside the tank.

The slosh frequencies and mode shapes vary with surface tension and free surface area. In low gravity, the highly 'wetting' liquids (those with very low surface tension) will have natural frequencies lower than those of non-wetting liquids. With baffles present, any number of sub-divisions of the interface might exist, and the varying free surface areas will give rise to a number of resonant frequencies which depend on fluid orientation. Thus, with a given fluid, prediction of only the range of fundamental slosh frequencies will be possible, along with the associated harmonics.

Summary

As a result of these considerations, it is expected that the baffling and aquisition systems required for dynamic control of the fluid will significantly alter the static configuration. Accurate prediction of static fluid orientation will be difficult, and prediction of specific slosh behavior impossible.

While the design of internal tank structures might also include fluid quantity measurement considerations, there will be a severe limit on the allowable scope of these design restrictions. Thus, any measurement system which is expected to remain accurate during and after vehicle accelerations must function while both the baffle and aquisition systems, as well as non-linear liquid-vapor interface configurations, are present. This is distinct from a simpler restriction on fluid location or orientation. Here, the measurements must remain insensitive to changes in shape or position with time.

It should be noted that generally, non-linearities in interface shape will not

persist, and there should exist some reasonable recovery time, after which such measurement difficulties will be significantly reduced. Salzman [50] and Sumner [51] have examined questions in liquid propellant reorientation in low gravity environments.

Appendix C

Dielectric Constant and Loss Tangent Data Used in Calculations

The calculation of predicted fill volume in the electromagnetic absorption methods presented in this thesis required knowledge of the dielectric constants and loss tangents of the test materials. For the resonance absorption experiments, kerosene and ethyl alcohol were used. In the case of the non-resonance experiment, these parameters were required for the modified PVC foam used to simulate liquid. The expression used to calculate predicted fill from measured Q values was derived in section 2.1,

$$V_{fl} = \frac{\kappa'_{fl} V_t (1/Q - 1/Q_{mt})}{\tan\delta + (\kappa'_{fl} - 1) / Q}$$

Ethyl Alcohol

The values of dielectric constant and loss tangent used for ethyl alcohol are shown below for the four resonance frequencies. These were calculated from the Debye model described in Appendix A,

$$\kappa = \kappa'_{\infty} + \frac{\kappa'_s - \kappa'_{\infty}}{1 + j\omega\tau}$$

where κ = relative complex permittivity or complex dielectric constant

κ'_s = static dielectric constant

κ'_{∞} = optical dielectric constant (frequency high enough to exclude dispersion)

τ = relaxation time

For ethyl alcohol, the values used were [52]

τ = 1.433e-10 sec

κ'_S = 25.07

κ'_∞= 4.10

The results are shown below.

mode	frequency (GHz)	κ'	κ''	tanδ
n = 8	8.209	4.48	2.79	0.663
n = 9	8.991	4.42	2.55	0.577
n = 10	10.007	4.36	2.30	0.528
n = 11	11.291	4.30	2.04	0.474

Kerosene

A search of the literature was done for loss tangent data on kerosene at these frequencies. Relaxation time for kerosene could not be found. Thus, the following values given by Von Hippel [53] were used for all three modes:

frequency (GHz)	κ'	κ''	tanδ
3.000	2.09	0.0094	.0045

Modified PVC Foam

Values of dielectric constant and loss tangent for this material were determined from measurements of capacitance C and quality factor Q for the empty and full parallel plate test tank, using a standard impedance bridge operating at 1 kHz. The definition of dielectric constant was used to calculate κ':

$$\kappa' = \frac{C_{full}}{C_{mt}} = \frac{81.5\ pF}{62\ pF} = 1.31 \pm 2\%$$

The loss tangent was determined by noting that total losses in the full tank are due to losses in the fluid and losses in the tank itself, or

$$\tan\delta_{total} = \tan\delta_{foam} + \tan\delta_{tank}$$

This may be written as

$$\frac{1}{Q_{total}} = \tan\delta_{foam} + \frac{1}{Q_{tank}}$$

Since $Q_{total} = Q_{full}$, and $Q_{tank} = Q_{mt}$,

$$\tan\delta_{foam} = \frac{1}{Q_{full}} - \frac{1}{Q_{mt}} = \frac{1}{32.5} - \frac{1}{313} = 0.028 \pm 9\%$$

The values found above for dielectric constant and loss tangent are in close agreement with those given by Von Hippel for Ensolite modified PVC foam at 20° C and f = 1 kHz [53].

References

1. TRW, "Feasibility Study of Positive Gauging Systems", Phase II Report, NASA contract # NAS9-6750, CR-65962, 1967.
2. Bendix Corp., "RF Quantity Gaging System for Cryogenic Applications", Development Assessment Report, Pub. # 4660A-70, Contract # NAS9-9661. June 1970.
3. Collier, R.S. et al., "Mass Quantity Gauging by RF Mode Analysis", NBSIR-73-318, June 1973.
4. Van Leuven, K. , Ball Aerospace, Denver. Personal Communication, March 1988.
5. Bendix Corp., "Studies to Determine the Feasibility of Various Techniques for Measuring Propellant Mass Aboard Orbiting Space Vehicles", Vol II, Phase B Final Report, N69-12144 (contract # NAS8-18039), June 1966 to June 1968.
6. Bendix Corp., "Studies to Determine the Feasibility of Various Techniques for Measuring Propellant Mass Aboard Orbiting Space Vehicles", Vol II, Phase B Interim Report, N68-22879, May 1968.
7. Ibid., Bendix Corp., N70-15211
8. Bendix Corp., "Design, Development, and Manufacture of a Breadboard Radio Frequency Mass Gauging System", Vol. 1: Phase B Final Report, N75-18546, NASA CR-120620, Nov. 1974.
9. Bendix Corp., "Design, Development, and Manufacture of a Breadboard Radio Frequency Mass Gauging System", Final Report, N76-12232, Nasa CR-144069, Dec. 1975.
10. Mord, A. et al, "Fluid Quantity Gaging Concept Selection Review", Presented Sept. 23 1986 at Johnson Space Center by Ball Aerospace Systems Division.
11. Von Hippel, A.R., "Dielectrics and Waves", Wiley & Sons, Inc., Library of Congress Catalog # 54-11020, 1954, p 39.
12. Montgomery, C.G., "Technique of Microwave Measurements", McGraw-Hill, 1947, pp 330-342.
13. Von Hippel, A.R., "Dielectric Materials and Applications", MIT Press, 1954, Chapter 2.
14. Buckley, F. and Maryott, A., "Tables of Dielectric Dispersion Data for Pure Liquids and Dilute Solutions", National Bureau of Standards Circular 589, 1958.
15. Maryott and Smith/National Bureau of Standards, "Tables of Dielectric Constants of Pure Liquids", NBS Circular 514, 1954.

16. Younglove, B.A./NBS, "Dielectric Constant of Compressed Gaseous and Liquid Oxygen", Journal of Research of the National Bureau of Standards, A76 no 1, p37 1972.
17. "Cryogenics and Industrial Gases", May/June 1974
18. Ely, J.F. and Straty, G.C., "Dielectric Constants and Molar Polarizabilities of Saturated and Compressed fluid Nitrogen", J. Chem. Phys. Vol. 61, No. 4, p. 1480 August 1974.
19. Pan, W.P. et al, "Dielectric Constants and Clausius-Mossotti Functions for Simple Liquid Mixtures: Systems Containing Nitrogen, Argon and Light Hydrocarbons", AIChE Journal, Vol. 21 No. 2, p.283, March 1975.
20. CRC Handbook of Physics and Chemistry, 1982.
21. Bendix Corp., "Studies To Determine the Feasibility of Various Techniques for Measuring Propellant Mass Aboard Obiting Space Vehicles", Vol 1: Phase A, Final report, N69-12143, NASA CR-98132, June 1966.
22. Daniel, V.V., "Dielectric Relaxation", Academic Press, New York, 1967. Library of Congress Cat # 67-28004, p.145.
23. Hill, N.E., et al, "Dielectric Properties and Molecular Behaviour", Van Nostrand Reinhold Co. New York, 1969, p299.
24. Kirkwood, J.G., "On the Theory of Dielectric Polarization", J. Chem. Phys. Vol 4, p 592, Sept. 1936.
25. Debye, P. "Polar Molecules", Chemical Catalog Co., New York, 1929.
26. Van Vleck, J. H., "Electric and Magnetic Susceptibility", Oxford 1932.
27. Frohlich, H., "Theory of Dielectrics, Dielectric Constant, and Dielectric Loss", Oxford 1986.
28. Van Vleck, J. H. and Wiesskopf, V. F., "On the Shape of Collision Broadened Lines", Rev. of Mod. Phys., Vol 17, No. 2 and 3, p227. April-July 1945
29. Maryott, A.A. and Birnbaum, G., "Microwave Absorption in Compressed Oxygen", J. Chem. Phys. Vol 32 No. 3, p686, March 1960.
30. Willis, W. L., "Electrical Conductivity of Some Cryogenic Fluids", Cryogenics J., p 279, October 1966.
31. White, E., "Electrical Conductivity of Low Dielectric Constant Liquids", S.M. Thesis, Chem. Eng., Massachusetts Institute of Technology, 1973.
32. Concus, P., Journal of Fluid Mechanics, Vol 34.

33. Reynolds, W. C. and Saterlee, H. M., "The Dynamic Behavior of Liquids", McGraw Hill, 1965. pp 397-399.
34. Ibid., p390.
35. Sumner, I.E., "Liquid Propellant Reorientation in a Low Gravity Environment", NASA TM-78969, 1978.
36. Slazman, J. A. and Masica, W. J. ,"Experimental Investigation of Liquid Propellant Reorientation", NASA TN-D-3789, 1967.
37. Abramson, H. N., "Dynamic Behavior of Liquids in Moving Containers", Applied Mechanics Revs. Vol 16, No. 7, pp 501-506, July 1963.
38. Stark, J.A., et al, "Low-g Fluid Behavior Technology Summaries", (General Dynamics/Convair NASA contract # NAS3-17814), NASA CR-134746, 1974
39. Bizzell, G.D., and Crane, G. E., "Numerical Simulation of Low Gravity Draining", Nasa CR-135004, 1976.
40. Hotchkiss, R.S., "Simulation of Tank Draining Phenomena with the NASA SOLA-VOF code. LA-8163-MS, US Dept of Energy, 1979
41. Cady, E.C, and Miyashiro, H.H.,"Filling of Orbital Fluid Management Systems", MDC-G7374, NASA CR-159405, 1978
42. Merino, F., et al, "Filling of Orbital Fluid Management Systems", CASD NAS-78-010 NASA CR-159405, 1978
43. Merino, F. et al, "Orbital Refill of Propulsion Vehicle Tankage", GDC-CRAD-80-001, NASA CR-1597222, 1980.
44. Abramson, H.N., et al, "Liquid Sloshing in Compartmented Cylindrical Tanks", ARS Journal, Vol. 32, No 6, pp 978-980, June 1962.
45. Abramson, H.N., et al, "Liquid Sloshing in Spherical Tanks", AIAA Journal, Vol 1, no 2, pp 384-389, Feb 1963.
46. Ibid. ref 44, 37.
47. Abramson, H.N., et al, "Some Measurements of Liquid Frequencies and Damping in Compartmented Cylindrical Tanks", AIAA Journal of Spacecraft and Rockets.
48. Dalzell, J.F. et al, "Studies of Ship Roll Stabilization Tanks", CN# 3926(00), Southwest Research Institute, Aug 1964.
49. Abramson, H.N., NASA TN D 1212.
50. Ibid ref 36.
51. Ibid ref 34
52. Ibid ref 14
53. Von Hippel, A. R., "Dielectric Materials and Applications", Wiley, New York, 1954, p 331.